

Title: Transcriptome and Proteome analysis of *Hemidactylus frenatus* during initial stages of tail regeneration.

Short title: Regeneration in gecko tail

Sai Pawan, Sarena Banu, Mohammed M Idris*

Sai Pawan, Project based Student, CSIR-CCMB, Uppal Road, Habsiguda, Hyderabad 500007. Email: n.sai.pawan325@gmail.com

Sarena Banu, Project Assistant, CSIR-CCMB, Uppal Road, Habsiguda, Hyderabad 500007. Email: sarena@ccmb.res.in

Mohammed M Idris, Senior Principal Scientist, CSIR-CCMB, Uppal Road, Habsiguda, Hyderabad 500007. Email: idris@ccmb.res.in

*Corresponding Author

Key words: Transcriptome; Proteome; Regeneration; Gecko; Network pathway

Abstract:

Epimorphic regeneration of appendages is a complex and complete phenomenon found in selected animals. *Hemidactylus frenatus*, the common house gecko has the remarkable ability to regenerate the tail tissue upon autotomy involving epimorphic regeneration mechanism. This study has identified and evaluated the molecular changes at gene and protein level during the regeneration of tail tissue. Based on next generation transcriptomics and *De novo* analysis the transcriptome and proteome library of the gecko tail tissue was generated. A total of 417 genes and 128 proteins were found to be associated with the regeneration of gecko tail tissue upon amputation at 1, 2 and 5-day post amputation against control, Odpa through differential analysis. The differentially expressed genes and proteins expressed a similar pattern for the commonly identified 36 genes/proteins involved in regeneration of the tail tissue. Similarly, the expression analysis of 50 genes were further validated involving real time PCR to authenticate the transcriptomics analysis. 327 genes/proteins identified from the study showed association for GP6 signaling pathway, Protein kinase A signaling, Telomerase signaling BAG2 signaling, paxiling signaling, VEGF signaling network pathways based on network pathway analysis. This study empanelled list of genes/proteins associated with tail tissue regeneration and its association for the mechanism.

INTRODUCTION

Regeneration is a sequential process specifically controlled by cellular mechanisms to repair or replace tissue or organ from an injury. The mass of undifferentiated cells (blastema) surrounding the injured tissue results in the formation of fully functional replica which enacts the phenomenon of epimorphic regeneration [1]. The ability to regenerate a full limb is absent in mammals but urodeles; teleost and amniotes have the propensity to replace limbs, spinal cords, nervous system, heart, tail and, other body parts [2]. To understand the mechanistic framework of regeneration, researchers have been majorly associated with urodeles amphibians [3]; teleost fishes [4]. Though amniotes i.e. lizards are closely related to mammals and other vertebrates, very little attention has been given to carry out regeneration on this organism [2], [5].

Lizard capacity to self-detach or amputate their tail in flight response from predators is known as the shedding of the tail or caudal autotomy [6]. These stages include exudation of excessive blood loss; minimizing muscle and bone tissue damage; controlled vascularisation; promotes wound epithelium and further unsegmented remodelling [7]. The Detachment of tail activates multiple cellular responses which spurts the blastema mediated cell proliferation, angiogenesis, remodelling and generating a replacement. Studies related to the patterning of successful regenerated autotomized tail or replica consists mainly of nerve cells networking, unsegmented cartilaginous, muscle cells, blood vessels and differential remodelling of cells which make this an interesting research to comprehend the cellular and molecular mechanisms associated with the development [8]–[10]. With the elucidation of the genes and their associated proteins involved in regeneration, there can be a possibility of understanding why in humans regeneration is restricted as compared to amniotes. This also might pave in giving insights into spinal injuries and the fabrication of replacement therapies [11]. Research on the regeneration of tail and its governing molecular mechanism in other lizard species like *Hemidactylus falviviridis* [12]; Green Anole [13-14]; and other vertebrates axolotl [15-17] have been carried out related to histology, proteomics and genomics [12 - 17]. Though many genes or proteins have been known still the underlying mechanisms of these molecules remains ambiguous. The present study is novel on this species “*Hemidactylus frenatus*” [18] commonly known as “Common House Gecko”. They are widely accessible, have a short life span and can be housed with minimal requirements and maintenance conditions. These species have been studied generally for their behavioural, habitat diversification and regenerative abilities [7], [19–22].

Lately, molecular and gene-specific studies focus on the role of genes like SOX9, PAX7, BMP, FGF, Wnt, MMP's which are usually associated with regeneration [23]. The expression of SOX9 during cartilage formation, PAX7 associating in tissue morphogenesis [24], BMP6 and other protein expressions were known [25, 26]. Constitutive expression and regulation of these genes have revealed a significant role during the developmental stages of regeneration. The slight alteration in the regulation of any of these genes results in a disrupted replacement. Thus, the activation and intricate cross-talk of these molecules during the process are still unaddressed and need to be better understood.

In this research, we sought to understand the molecular mechanisms of lost tail regeneration process during preliminary stages (0dpa, 1dpa, 2dpa, and 5dpa) which would further help in understanding the molecular cues and the genes or proteins associated with the process. The initial stages (i.e. wound healing) are responsible for wound epithelium and initiating apical epidermal cap (AEC) which regulates blastema formation [7]. Though, during the initial stages, the activity of the molecules regulating the regeneration process is not known which is crucial to instigate the replacement of the lost tissue. The study of prelude stages of regeneration has been carried out in zebrafish caudal fin [27]; other species [28] and shown changes in the regulation of genes or proteins. However, this stage-specific study has not been carried out in this species and as it is necessary for deciphering the crucial molecules which kick starts the regenerative mechanism in these amniotes. Here, we list out the involvement of crucial genes or proteins and their differential expression associated with the molecular processes in tail regeneration through transcriptome and proteome approaches.

MATERIALS AND METHODS

1. Animal and Sample Collection

The lizard, *Hemidactylus frenatus* were collected and maintained in a well-ventilated cage with adequate proper diet, optimum temperature (~25°C) and the 12 hours light and dark cycle. Amputation of tail tissue were performed on batches of animals using sterile scalpel blade. Regenerating tail tissues preceding the amputation site were collected for each time points (0dpa, 1dpa, 2dpa, 5dpa) of (n=5). The collected control and regenerating tail tissues were washed with 1X phosphate-buffered saline (PBS), pooled and snap-frozen in liquid nitrogen and was store at -70°C until use. The animal experiment were performed in accordance with the protocol approved by the Institutional animal ethics committee of Centre for Cellular and Molecular Biology (IAEC/CCMB/Protocol # 66/2014).

2. Total RNA Isolation

Total RNA was extracted from the tissues of each time points using RNA isoPlus Reagent (Takara Bio, CA, USA) following the manufacturer's protocol. The RNA yield and purity was calculated using NanoDrop 2000 Thermo fisher and gel analysis.

3. NGS transcriptomic analysis

The total RNA transcripts of each time point tissues were obtained based on next generation sequencing (NGS) analysis involving Illumina HiSeq 2000 [28]. All the transcripts obtained commonly from all the tissues were further assembled for De novo transcriptome analysis and functional annotation against non-redundant reptilian database using blastx [28]. Both the known and unknown gene sequences obtained from the NGS analysis were tabulated and submitted to NCBI and obtained accession number. Also the genes were translated for obtaining protein database.

4. Differential expression analysis

The transcripts were further analysed for their expression level using FPKM and analysed for differential expression level on 1, 2 and 5dpa time points against 0dpa as control [28]. Differentially expressed transcripts having at least 1.0 log fold change in any one of their regenerating time points were considered for the study.

5. Real Time PCR (RT-PCR) analysis

Validation of fifty most significantly expressed genes having more than 2 log fold changes in any of its time points were selected for RTPCR analysis. Primers were designed using Primer3 software. Amplification of 14-3-3 protein zeta/delta isoform X1 and NADH dehydrogenase 1 alpha sub complex subunit 11 were used as housekeeping gene. RTPCR were performed in biological and technical replicates for each genes from the cDNA synthesized from 1 µgms total RNA using Takara SYBR green assay master mix. The relative expressions of the genes were estimated based on the RTPCR Ct value against control (0dpa) as the baseline.

6. Protein extraction and iTRAQ analysis

The total protein from the control and regenerating tail tissues were extracted using protein extraction buffer (7M urea, 2M thiourea, 18mM Tris-HCl, 4% CHAPS, 14mM Trizmabase, 2 Tablets EDTA protease Inhibitor, Triton X 0.2%, 50mM DTT) upon homogenization and sonication [27, 29]. The proteins were quantified using Amido black method [30] against BSA as standard. iTRAQ based quantitative proteomics analysis was performed in duplicates between the control (0dpa) and regenerating time points (1dpa, 2dpa and 5dpa) by loading 50 µg of total proteins in a 10% SDS-PAGE gel. The gel was stained, destained, documented and fractionated into four sequential groups. The gel fractions were washed; trypsin digested, labelled with isobaric tags iTRAQ 4-plex labelling and purified with the help of C-18 spin columns (Thermo Scientific). The purified/labelled peptides were vacuum dried and constituted in 5% acetonitrile (ACN) and 0.2% formic acid to the peptides for the LCMS/MSMS analysis [28]. The LCMS/MSMS run was performed in Orbitrap Velos Nano analyzer (Thermo) involving High Collision Dissociation (HCD) mode of acquisition with 50% normalized collision energy. The raw files were analyzed with Sequest HT proteome discoverer 1.4 (Thermo Scientific), with 1% FDR using percolator and XCorr (Score Vs Charge) against the NGS generated lizard database. All the proteins, in duplicates, were analyzed against the control (0dpa). Differentially regulated expression by more than 1-log fold changes were selected as proteins associated with regeneration.

7. Heat Map and Network Pathway analysis :

All the differentially expressed genes and proteins were analysed for the heat map analysis involving heatmapper portal (www.heatmapper.ca) towards elucidating the hierarchical cluster analysis of the genes/proteins and the time points. The association of these genes /

proteins were also analyzed for the association in network pathways based on Ingenuity pathway analysis (IPA).

Results:

Transcriptomic analysis of regeneration:

A total of 42551 transcripts sequences were obtained from the NGS analysis of all four tail tissue samples. All the sequences were obtained from a total of ~ 30 million reads from each sample. De novo and functional annotation yielded 39953 transcripts with highest similarity with *Gekko japonicas* (41.3%) and no blast hit (49%) to any reptilian database. The transcripts were submitted to NCBI and obtained accession number (SUB6511228). The transcripts were further translated to obtain the protein sequence database for proteomic analysis.

A total of 417 genes were found to be associated with regeneration of gecko tail tissue for having at least one log fold change in one of its regenerating time points significantly. 254 genes were selected for further analysis such as heat map and network pathway analysis for having their expression pattern in all their regenerating time points (Figure 1a; Table 1). Genes such as Erythrocyte membrane protein (EPB41), retinoic acid receptor responder protein 1 and few uncharacterized proteins were found to be upregulated for having more than 5 log fold upregulation of gene expression. Similarly, Ryanodine receptor 1, Myosin 1B were found to be regulated austere (Table 1). Clustal hierarchical heat map analysis of the differentially regulated genes revealed group of genes which were undergoing upregulation at 1dpa where found to be down regulated at 2 and 5dpa and vice versa with down regulated genes at 1dpa (Figure 1a). The analysis further reveals that 1dpa expression is out rooted with clustered 2 and 5dpa based on cluster analysis for the three regenerating time points against the control tissue expression.

Proteomic analysis of regeneration:

A total of 128 proteins were found to be differentially regulated during the early stage of regeneration of gecko tail tissues for having minimum of one log fold changes significantly (Table 2). Annexin A2, Cathepsin B and MYL1 were some of the major upregulated proteins and Myozenin, GST and GSK were the major down regulated proteins. A total of 36 proteins which were differentially regulated at the proteome level were also found to be differentially regulated at gene level based on the transcriptomics analysis (Figure 1c). Like transcriptome expression pattern, proteome expressions were also found to be associated with regeneration by clustering of 2 and 5dpa (Figure 1d). All the proteins which were upregulated

at 1 dpa were found to be down regulated either at 2 or 5 dpa. Similarly all the down regulated proteins were found to be upregulated at 2 or 5 dpa.

Validation of gene expression:

RTPCR analysis of 50 genes selected for the validation study showed significant differential expression of the genes for the regeneration mechanism (Figure 2a and 2b). Almost all the up and down regulated genes which were identified from the transcriptomic analysis were found to be associated with regeneration through differential regulation based on RTPCR analysis (Figure 1b). Heat map analysis of the gene expression based on RTPCR analysis also showed association of 2 and 5 dpa as cluster against 1 dpa expression.

Network Pathway Analysis:

A total of 327 genes/proteins were mapped by the Ingenuity Pathway analysis software for the network and pathway analysis. The major molecular and cellular functions associated with the differentially regulated genes/proteins during regeneration are cellular assembly & organization, cellular compromise, cellular functions & maintenance and Cellular development. The major physiological system development and functions associated with regeneration mechanism are skeletal & muscular system development, embryonic development, organ development and tissue development.

The most significant canonical pathways which were found to be associated with genes/proteins were GP6 signaling pathway, Protein kinase A signaling, Telomerase signaling BAG2 signaling, paxiling signaling, VEGF signaling and various metabolic pathways (Figure 3a). The major network pathways associated with the identified and dysregulated genes/proteins based on differential analysis includes Cell morphology and Embryonic development (Figure 3b), Cellular assembly and organization (Figure 3c), Organ and organismal development (Figure 3d) and Skeletal and Muscular development (Figure 3e).

Discussion:

This study aimed to evaluate the genomic and proteomic changes during the early stages of tail tissue regeneration in house lizard. Zebrafish and other invertebrates have been extensively studied for understanding the epimorphic regeneration [27, 28] at the genomic and proteomic level. This study has been done similar to our earlier study using the house gecko as the model animal.

The study not only mapped the transcriptome of gecko tail tissue but also identified the list of genes and proteins involved in regeneration of the tail tissue upon amputation. Several known and unknown genes/proteins which were identified in this study were also involved in epimorphic regeneration of caudal fin tissue of zebrafish [27]; arm of brittle star [28] and tail of *Hemidactylus flaviviridis* [12]. 417 genes and 134 proteins were identified as differentially regulated in the regenerating tissues. Validation of 50 genes identified from the transcriptomic analysis confirms the differential regulation of the genes for the biomechanism of regeneration, which is also evident from the hierarchical heat map analysis of the transcriptome and proteome and RTPCR expression analysis.

The canonical pathway associated with the differentially expressed genes/proteins are mostly signalling and metabolic pathways. The major network pathways associated with the tail tissue regeneration are Cell morphology, embryonic development and skin development (Figure 3b) involving 26 genes/proteins of the study such as DSC1, DSC2, GPI, DSP and keratin proteins. Similarly, 25 genes/proteins, such as ADRM1, APOA1, ASPH, ATP2A1 were associated with Cellular assembly and organization (Figure 3c). Organ and organismal development network pathway (Figure 3d) were associated with 28 genes/proteins such as ACTC1, ACTG1, BIN1, CAPZA2 and CAPZB. Skeletal and muscular system development network pathway (Figure 3e) was associated with 25 genes/proteins such as CBR1, DLX3, EEF1B2 and DLX3. This study has identified and associated various genes/proteins and their network pathways for the tail tissue regeneration of lizard which were also found to be associated with epimorphic regeneration of organs in other animals as in zebrafish [27] and echinoderms [28]. Further understanding of the differential expressed genes/proteins and their regulation might lead to better insight in understanding the regeneration of the gecko tail.

Acknowledgements:

This work was supported by CSIR-YSA Project. The authors are grateful to Noorul Fowzia for critically reviewing the manuscript.

REFERENCES:

1. Londono, R., Sun, A.X., Tuan, R.S. and Lozito, T.P., 2018. Tissue repair and epimorphic regeneration: An overview. *Current pathobiology reports*, 6(1), 61-69.
2. Jacyniak, K., McDonald, R.P. and Vickaryous, M.K., 2017. Tail regeneration and other phenomena of wound healing and tissue restoration in lizards. *Journal of Experimental Biology*, 220(16), 2858-2869.
3. McCusker, C. and Gardiner, D.M., 2011. The axolotl model for regeneration and aging research: a mini-review. *Gerontology*, 57(6), 565-571.
4. Gemberling, M., Bailey, T.J., Hyde, D.R. and Poss, K.D., 2013. The zebrafish as a model for complex tissue regeneration. *Trends in Genetics*, 29(11), 611-620.
5. Alibardi, L., 2010. Morphological and cellular aspects of tail and limb Regeneration in Lizards. A model system with implications for tissue regeneration in mammals. *Adv Anat Embryol Cell Biol*. 207, 1-109.
6. Clause, A.R. and Capaldi, E.A., 2006. Caudal autotomy and regeneration in lizards. *Journal of Experimental Zoology Part A: Comparative Experimental Biology*, 305(12), 965-973.
7. Gilbert, E.A.B., Delorme, S.L. and Vickaryous, M.K., 2015. The regeneration blastema of lizards: an amniote model for the study of appendage replacement. *Regeneration*, 2(2), 45-53.
8. Delorme, S.L., Lungu, I.M. and Vickaryous, M.K., 2012. Scar-free wound healing and regeneration following tail loss in the leopard gecko, *Eublepharis macularius*. *The Anatomical Record: Advances in Integrative Anatomy and Evolutionary Biology*, 295(10), 1575-1595.
9. McLean, K.E. and Vickaryous, M.K., 2011. A novel amniote model of epimorphic regeneration: the leopard gecko, *Eublepharis macularius*. *BMC developmental biology*, 11(1), p.50.
10. Payne, S.L., Peacock, H.M. and Vickaryous, M.K., 2017. Blood vessel formation during tail regeneration in the leopard gecko (*Eublepharis macularius*): the blastema is not avascular. *Journal of morphology*, 278(3), 380-389.
11. Simkin, J., Sammarco, M.C., Dawson, L.A., Schanes, P.P., Yu, L. and Muneoka, K., 2015. The mammalian blastema: regeneration at our fingertips. *Regeneration*, 2(3), 93-105.

12. Murawala, H., Ranadive, I., Patel, S., Desai, I. and Balakrishnan, S., 2018. Protein expression pattern and analysis of differentially expressed peptides during various stages of tail regeneration in *Hemidactylus flaviviridis*. *Mechanisms of development*, 150, 1-9.
13. Fisher, R.E., Geiger, L.A., Stroik, L.K., Hutchins, E.D., George, R.M., Denardo, D.F., Kusumi, K., Rawls, J.A. and Wilson-Rawls, J., 2012. A histological comparison of the original and regenerated tail in the green anole, *Anolis carolinensis*. *The Anatomical Record: Advances in Integrative Anatomy and Evolutionary Biology*, 295(10), 1609-1619.
14. Hutchins, E.D., Markov, G.J., Eckalbar, W.L., George, R.M., King, J.M., Tokuyama, M.A., Geiger, L.A., Emmert, N., Ammar, M.J., Allen, A.N. and Siniard, A.L., 2014. Transcriptomic analysis of tail regeneration in the lizard *Anolis carolinensis* reveals activation of conserved vertebrate developmental and repair mechanisms. *PloS one*, 9(8), p.e105004.
15. Slack, J.M.W., 1982. Protein synthesis during limb regeneration in the axolotl. *Development*, 70(1), 241-260.
16. Kozhemyakina, E., Lassar, A.B. and Zelzer, E., 2015. A pathway to bone: signaling molecules and transcription factors involved in chondrocyte development and maturation. *Development*, 142(5), 817-831.
17. Rao, N., Jhamb, D., Milner, D.J., Li, B., Song, F., Wang, M., Voss, S.R., Palakal, M., King, M.W., Saranjami, B. and Nye, H.L., 2009. Proteomic analysis of blastema formation in regenerating axolotl limbs. *BMC biology*, 7(1), p.83.
18. Patel, H., Naik, V. and Tank, S.K., 2016. The Common House Gecko, *Hemidactylus frenatus* Schlegel in Dumeril & Bibron 1836 (Reptilia: Gekkonidae) in Gujarat, India. *IRCF Reptiles & Amphibians*, 23, 178-182.
19. Rakhmiyati, R. and Luthfi, M.J.F., 2018. Alizarin Red S-Alcian Blue Staining for Regenerated tail of Common House Gecko (*Hemidactylus frenatus*). *Biology, Medicine, & Natural Product Chemistry*, 7(2), 57-59.
20. Rakhmiyati, R. and Luthfi, M.J., 2016. Histological Study of Common House Gecko (*Hemidactylus frenatus*) Regenerated Tail. *Biology, Medicine, & Natural Product Chemistry*, 5(2), 49-53.
21. Carranza, S. and Arnold, E.N., 2006. Systematics, biogeography, and evolution of *Hemidactylus* geckos (Reptilia: Gekkonidae) elucidated using mitochondrial DNA sequences. *Molecular phylogenetics and evolution*, 38(2), 531-545.

22. Maginnis, T.L., 2006. The costs of autotomy and regeneration in animals: a review and framework for future research. *Behavioral Ecology*, 17(5), 857-872.
23. Poss, K.D., Shen, J., Nechiporuk, A., McMahon, G., Thisse, B., Thisse, C. and Keating, M.T., 2000. Roles for Fgf signaling during zebrafish fin regeneration. *Developmental biology*, 222(2), 347-358.
24. Liu, Y., Zhou, Q., Wang, Y., Luo, L., Yang, J., Yang, L., Liu, M., Li, Y., Qian, T., Zheng, Y. and Li, M., 2015. Gekko japonicus genome reveals evolution of adhesive toe pads and tail regeneration. *Nature communications*, 6, p.10033.
25. Yu, Y., Tang, J., Su, J., Cui, J., Xie, X. and Chen, F., 2019. Integrative analysis of microRNAome, transcriptome, and proteome during the limb regeneration of *Cynops orientalis*. *Journal of proteome research*, 18(3), 1088-1098.
26. Quint, E., Smith, A., Avaron, F., Laforest, L., Miles, J., Gaffield, W. and Akimenko, M.A., 2002. Bone patterning is altered in the regenerating zebrafish caudal fin after ectopic expression of sonic hedgehog and *bmp2b* or exposure to cyclopamine. *Proceedings of the National Academy of Sciences*, 99(13), 8713-8718.
27. Saxena, S., Singh, S.K., Lakshmi, M.G.M., Meghah, V., Bhatti, B., Swamy, C.V.B., Sundaram, C.S. and Idris, M.M., 2012. Proteomic analysis of zebrafish caudal fin regeneration. *Molecular & Cellular Proteomics*, 11(6), M111-014118.
28. Purushothaman, S., Saxena, S., Meghah, V., Swamy, C.V.B., Ortega-Martinez, O., Dupont, S. and Idris, M., 2015. Transcriptomic and proteomic analyses of *Amphiura filiformis* arm tissue-undergoing regeneration. *Journal of proteomics*, 112, 113-124.
29. Singh, S.K., Lakshmi, M.G.M., Saxena, S., Swamy, C.V.B. and Idris, M.M., 2011. Proteome profile of zebrafish caudal fin based on one-dimensional gel electrophoresis LCMS/MS and two-dimensional gel electrophoresis MALDI MS/MS analysis. *Journal of separation science*, 34(2), 225-232.
30. Weissmann, S.W., 1973. A rapid for sensitive, the in dilute and Specific of method protein determination solution. *Anal Biochem*, 56, 502-514.

Legends:

Figure 1: a. Heat map expression of *Hemidactylus frenatus* transcript during tail tissue regeneration b. Heat map expression of various genes differentially regulated during regeneration based on RTPCR analysis; c. Venn diagram for number genes identified from Transcriptomics, proteomics and Real time PCR based gene expression analysis D. Heat map expression of differentially expression proteins which are associated with tail regeneration.

Figure 2: RTPCR analysis of differentially expressed transcripts. a. Gel image of all the 50 genes along with housekeeping gene. b. Bar diagram of expression visualising the up and down regulation of the genes.

Figure 3: a. Canonical Pathway associated with the differentially expressed genes/proteins for tail regeneration; b. Cell morphology and Embryonic development network pathway; c. Cellular assembly and organization network pathway; d. Organ and organismal development network pathway; e. Skeletal and Muscular development network pathway.

Table 1: List of differentially expressed genes based on NGS transcriptomic analysis. Accession, description, symbol, 1dpa fold changes, 2dpa fold changes, 5dpa fold changes, 1dpa p value, 2dpa p values and 5dpa p values were shown in each column.

Table 2: List of differentially expressed protein based on iTRAQ proteomic analysis. Accession, description, symbol, No of peptides identified, peptide sequence matches, 1dpa fold changes, 2dpa fold changes, 5dpa fold changes, 1dpa SEM, 2dpa SEM and 5dpa SEM were shown in each column.

Table 1: List of differentially expressed genes based on NGS transcriptomic analysis. Accession, description, symbol, 1dpa fold changes, 2dpa fold changes, 5dpa fold changes, 1dpa p value, 2dpa p values and 5dpa p values were shown in each column.

S. No	Accession	Description	Symbol	1dpa FC	2dpa FC	5dpa FC	1dpa pval	2dpa pval	5dpa pval
1	TRINITY_DN30805_c0_g3_i3	Similar to Gekko japonicus uncharacterized LOC107120650	N/A	-3.7	-3.7	-6.1	0.0	0.0	0.1
2	TRINITY_DN38093_c1_g1_i2	ADAM metallopeptidase domain 9 (ADAM9), mRNA like	ADAM9I	-1.7	-4.6	-6.1	0.2	0.0	0.1
3	TRINITY_DN24480_c0_g2_i1	3-hydroxybutyrate dehydrogenase, type 2 (BDH2), transcript variant X2, mRNA	BDH2	-1.0	3.6	2.2	1.0	0.0	0.5
4	TRINITY_DN30186_c0_g1_i6	Prolyl 4-hydroxylase, beta polypeptide (P4HB), transcript variant X1, mRNA	P4HB	-1.0	3.8	5.5	1.0	0.0	0.1
5	TRINITY_DN19868_c1_g5_i1	Transmembrane protein 128 (TMEM128), mRNA	TMEM128	-0.7	-2.9	-7.4	0.6	0.1	0.0
6	TRINITY_DN34808_c4_g3_i1	Isolate DB198 basic leucine zipper and W2 domain-containing protein 1 (BZW1) gene	BZW1	-0.7	-3.5	-5.1	0.6	0.0	0.1
7	TRINITY_DN20768_c1_g1_i1	Ankyrin repeat domain 23 (ANKRD23), mRNA	ANKRD23	-0.4	-3.1	-4.7	0.8	0.0	0.1
8	TRINITY_DN36827_c0_g1_i3	Uncharacterized	N/A	-0.4	-4.8	-5.3	0.8	0.0	0.1
9	TRINITY_DN22212_c0_g1_i1	HOXD13 (HoxD13) gene	HOXD13	-0.1	-5.3	-6.9	0.9	0.0	0.0
10	TRINITY_DN26064_c0_g1_i1	FGB gene for beta-fibrinogen,	FGB	-0.1	-7.6	-9.2	0.9	0.0	0.0
11	TRINITY_DN24344_c0_g1_i2	Poly(A) binding protein interacting protein 2 (PAIP2)	PAIP2	0.0	3.7	2.4	1.0	0.0	0.5
12	TRINITY_DN34394_c2_g5_i1	Plakophilin-1-like	PKP1	0.0	-3.4	-4.6	1.0	0.0	0.1
13	TRINITY_DN24813_c0_g1_i2	Similar to Gekko japonicus uncharacterized LOC107121858	N/A	0.2	-5.0	-3.6	0.9	0.0	0.2
14	TRINITY_DN30559_c0_g1_i5	Serine/arginine-rich splicing	SRSF2	0.6	3.4	3.2	0.7	0.0	0.3

		factor 2 (SRSF2)							
15	TRINITY_DN34182_c1_g1_i1	Myosin-4-like	MYH4	0.9	-1.3	-8.5	0.5	0.4	0.0
16	TRINITY_DN27889_c0_g3_i1	Peroxisome proliferator-activated receptor alpha (PPARA)	PPARA	0.9	-4.4	-4.0	0.5	0.0	0.2
17	TRINITY_DN26747_c2_g1_i4	Similar to Gekko japonicus uncharacterized LOC107111273	N/A	0.9	-5.9	-1.9	0.5	0.0	0.5
18	TRINITY_DN19823_c3_g3_i1	Similar to Gekko japonicus uncharacterized LOC107117390	N/A	1.0	-5.5	-5.1	0.5	0.0	0.1
19	TRINITY_DN30281_c0_g4_i1	Prosaposin-like	PSAP	1.1	-5.1	-6.7	0.4	0.0	0.1
20	TRINITY_DN20187_c0_g2_i1	Serine peptidase inhibitor, Kunitz type 1 (SPINT1)	SPINT1	1.2	-3.3	-3.9	0.4	0.0	0.2
21	TRINITY_DN27754_c0_g2_i2	Cytosolic arginine sensor for mTORC1 subunit 1	mTORC1	3.9	2.3	-0.6	0.0	0.3	1.0
22	TRINITY_DN26638_c0_g3_i1	Angiopoietin like 7 (angptl7)	angptl7	4.0	3.0	-0.6	0.0	0.1	1.0
23	TRINITY_DN36464_c1_g1_i2	Chromosome unknown open reading frame, human C8orf22 like	C8orf22l	4.8	3.9	-0.6	0.0	0.0	1.0
24	TRINITY_DN23291_c3_g5_i1	Uncharacterized	N/A	7.8	8.3	4.3	0.0	0.0	0.2
25	TRINITY_DN38002_c1_g2_i2	Calsequestrin-1	CASQ1	-7.1	-1.6	-8.6	0.0	0.3	0.0
26	TRINITY_DN22817_c0_g2_i5	myosin-1B-like isoform X4	MYO1B	-6.5	-3.0	-5.7	0.0	0.1	0.1
27	TRINITY_DN32422_c0_g2_i3	myosin-1B-like isoform X8	MYO1B	-5.9	-2.3	-3.0	0.0	0.1	0.3
28	TRINITY_DN30722_c0_g2_i4	muscle-related coiled-coil protein	MURC	-3.9	-1.9	-2.9	0.0	0.2	0.3
29	TRINITY_DN34854_c2_g1_i3	UAP56-interacting factor-like	FYTTD1	-3.9	-1.1	-1.7	0.0	0.5	0.5
30	TRINITY_DN30393_c0_g2_i1	keratin, type II cytoskeletal 4-like	KRT4	-3.5	-4.3	-4.1	0.0	0.0	0.2
31	TRINITY_DN38213_c1_g1_i5	MEF2-activating motif and SAP domain-containing transcriptional regulator	MEF2	-2.7	-3.7	-4.3	0.1	0.0	0.2
32	TRINITY_DN22052_c0_g2_i6	osteocalcin	BGLAP	-2.7	-4.0	-4.0	0.1	0.0	0.0
33	TRINITY_DN36268_c0_g1_i2	myomegalin isoform X2	pde4dip	-2.2	-3.8	-4.4	0.1	0.0	0.2
34	TRINITY_DN38093_c1_g1_i3	disintegrin and metalloproteinase	ADAM9	-2.2	-3.6	-1.5	0.1	0.0	0.6

		domain-containing protein 9							
35	TRINITY_DN36578_c0_g1_i4	ryanodine receptor 2	RYR2	-2.2	-4.2	-4.8	0.1	0.0	0.1
36	TRINITY_DN26958_c0_g3_i1	homeobox protein DLX-3	DLX3	-2.1	-3.4	-3.4	0.1	0.0	0.1
37	TRINITY_DN37846_c0_g1_i3	desmoplakin isoform X1	DSP	-3.7	-4.0	-4.6	0.0	0.0	0.2
38	TRINITY_DN22305_c3_g3_i2	NEDD8	NEDD8	-1.6	3.5	3.6	0.6	0.0	0.2
39	TRINITY_DN38176_c1_g2_i2	uricase-like	UOX	-1.5	-5.1	-5.1	0.3	0.0	0.0
40	TRINITY_DN22220_c0_g1_i1	afadin isoform X6	AFDN	-1.4	-3.7	-4.3	0.3	0.0	0.2
41	TRINITY_DN38238_c1_g1_i1	nebulin isoform X12	NEB	-1.3	-6.2	-4.3	0.3	0.0	0.0
42	TRINITY_DN28089_c0_g3_i1	vesicle-associated membrane protein-associated protein B/C	VAPB	-1.2	-3.8	-4.4	0.4	0.0	0.2
43	TRINITY_DN25660_c0_g5_i1	17-beta-hydroxysteroid dehydrogenase 14-like	HSD17B14	-3.2	-5.8	-7.4	0.0	0.0	0.0
44	TRINITY_DN36527_c0_g2_i1	death-associated protein-like 1	DAPL1	-0.8	-3.8	-0.8	0.6	0.0	0.1
45	TRINITY_DN31814_c0_g2_i2	leukocyte elastase inhibitor-like	SERPINB1	-0.7	-6.2	-0.7	0.6	0.0	0.0
46	TRINITY_DN21431_c0_g2_i3	poly(rC)-binding protein 2 isoform X11	PCBP2	-0.3	3.8	3.9	1.0	0.0	0.2
47	TRINITY_DN26467_c0_g1_i1	NHP2-like protein 1	SNU13	0.0	4.0	3.8	1.0	0.0	0.2
48	TRINITY_DN37657_c1_g4_i2	p53 apoptosis effector related to PMP-22	PMP-22	0.0	-3.9	-4.5	1.0	0.0	0.2
49	TRINITY_DN35820_c0_g1_i2	desmin	DES	0.4	-2.5	-7.3	0.8	0.1	0.0
50	TRINITY_DN26831_c0_g2_i3	shematin-like protein 2	SHEM1	0.6	-6.8	-7.8	0.7	0.0	0.0
51	TRINITY_DN34867_c2_g1_i3	methyltransferase-like protein 7A	METTL7A	1.3	-3.8	-4.4	0.3	0.0	0.2
52	TRINITY_DN32563_c0_g2_i2	DDB1- and CUL4-associated factor 6 isoform X1	DCAF6	1.5	3.5	3.2	0.3	0.0	0.3
53	TRINITY_DN19443_c0_g2_i1	C-C motif chemokine 5-like	CCL5	1.9	3.7	2.2	0.2	0.0	0.5
54	TRINITY_DN27678_c0_g3_i1	retinol-binding protein 5	RBP5	2.2	3.4	1.9	0.1	0.0	0.5
55	TRINITY_DN36609_c1_g2_i3	mitogen-activated protein kinase kinase kinase 7 isoform X2	MAP3K7	3.1	2.7	2.2	0.0	0.1	0.5
56	TRINITY_DN35430_c0_g1_i4	proteasomal ubiquitin receptor ADRM1	ADRM1	3.5	3.6	3.6	0.0	0.1	0.8

57	TRINITY_DN23823_c0_g2_i4	AN1-type zinc finger protein 2A	ZFAND2A	3.6	3.0	3.0	0.0	0.1	0.8
58	TRINITY_DN23648_c1_g2_i1	cathelicidin-related peptide Oh-Cath-like	CATH	3.7	4.8	-0.6	0.0	0.0	1.0
59	TRINITY_DN24620_c0_g5_i1	phospholipase A2 inhibitor subunit gamma B-like	PLA2	3.9	4.4	1.3	0.0	0.0	0.7
60	TRINITY_DN36845_c0_g1_i4	alpha-actinin-3	ACTN3	4.9	5.1	2.4	0.0	0.0	0.4
61	TRINITY_DN31052_c0_g1_i2	retinoic acid receptor responder protein 1	RARRES1	5.0	2.9	1.0	0.0	0.1	0.8
62	TRINITY_DN23991_c0_g2_i1	PCNA-associated factor	PCLAF	3.9	3.9	5.2	1.0	0.0	0.1
63	TRINITY_DN27770_c0_g4_i1	14-3-3 protein sigma	SFN	-1.6	-5.7	-5.3	0.2	0.0	0.1
64	TRINITY_DN20642_c2_g2_i3	39S ribosomal protein L17, mitochondrial	MRPL17	-3.9	1.3	2.3	0.0	0.4	0.4
65	TRINITY_DN24484_c0_g4_i1	40S ribosomal protein S11	RPS11	-3.5	1.0	1.7	0.0	0.5	0.5
66	TRINITY_DN26256_c1_g1_i6	40S ribosomal protein S12	RPS12	-0.2	0.9	-8.3	0.9	0.5	0.0
67	TRINITY_DN20830_c0_g5_i1	40S ribosomal protein S24 isoform X2	RPS24	0.1	0.8	-8.6	1.0	0.6	0.0
68	TRINITY_DN23044_c0_g1_i1	40S ribosomal protein S25	RPS25	-3.0	0.9	1.8	0.0	0.5	0.5
69	TRINITY_DN24077_c0_g2_i3	60S ribosomal protein L18	RPL18	-3.7	1.3	1.8	0.0	0.4	0.5
70	TRINITY_DN20257_c0_g1_i4	60S ribosomal protein L35a	RPL35A	0.2	1.6	-7.4	0.9	0.3	0.0
71	TRINITY_DN35974_c0_g2_i1	A.superbus venom factor 1-like	AVF1	0.0	3.6	3.6	1.0	0.0	0.2
72	TRINITY_DN31002_c0_g2_i2	actin, alpha cardiac muscle 1	ACTC1	0.8	-0.9	-8.0	0.6	0.5	0.0
73	TRINITY_DN35992_c0_g2_i1	adenylosuccinate synthetase isozyme 1	ADSSL1	-1.5	-3.4	-3.0	0.3	0.0	0.3
74	TRINITY_DN37906_c2_g1_i5	alpha-enolase isoform X1	ENO1	-3.9	0.1	-0.6	0.0	1.0	0.8
75	TRINITY_DN34147_c2_g1_i3	alpha-sarcoglycan isoform X2	SGCA	-3.2	0.3	-0.2	0.0	0.9	1.0
76	TRINITY_DN34179_c3_g3_i1	annexin A2	ANXA2	-0.5	0.3	-8.5	0.7	0.9	0.0
77	TRINITY_DN25783_c2_g1_i5	aspartyl/asparaginyl beta-hydroxylase isoform X3	ASPH	-3.8	1.4	0.1	0.0	0.4	1.0
78	TRINITY_DN30115_c0_g2_i10	ATP synthase F(0) complex subunit C1, mitochondrial	ATP5MC1	-4.3	0.8	1.5	0.0	0.6	0.6

79	TRINITY_DN26389_c0_g5_i1	ATP synthase F(0) complex subunit C2, mitochondrial	ATP5MC2	-3.6	1.1	1.0	0.0	0.5	0.7
80	TRINITY_DN22271_c0_g2_i2	ATP synthase subunit d, mitochondrial	ATP5PD	-4.1	0.9	2.3	0.0	0.5	0.4
81	TRINITY_DN21311_c1_g1_i1	avidin-like	AVD	3.1	2.5	4.7	0.0	0.1	0.1
82	TRINITY_DN33064_c0_g1_i3	bax inhibitor 1	TMBIM6	-4.5	1.0	0.8	0.0	0.5	0.8
83	TRINITY_DN25564_c1_g2_i5	bcl-2-like protein 10	BCL2L10	3.5	2.3	0.0	0.0	0.2	1.0
84	TRINITY_DN32628_c1_g1_i1	beta-2-microglobulin isoform X1	B2M	-0.4	-0.3	-6.7	0.8	0.8	0.0
85	TRINITY_DN37021_c1_g1_i1	beta-enolase	ENO3	-0.7	-1.0	-8.5	0.7	0.5	0.0
86	TRINITY_DN29143_c0_g1_i3	betaine--homocysteine S-methyltransferase 1	BHMT	3.8	2.0	-2.9	0.0	0.2	0.4
87	TRINITY_DN32939_c2_g1_i1	CCAAT/enhancer-binding protein delta	CEBPD	-3.5	-1.1	1.2	0.0	0.4	0.7
88	TRINITY_DN32564_c0_g3_i6	CD63 antigen	CD63	-3.6	1.2	1.7	0.0	0.4	0.5
89	TRINITY_DN24309_c1_g1_i2	claw keratin-like	CKER1	3.6	-7.5	-4.1	0.0	0.0	0.2
90	TRINITY_DN27033_c0_g1_i5	cold-inducible RNA-binding protein isoform X1	CIRBP	-5.4	-0.2	-0.2	0.0	0.9	0.9
91	TRINITY_DN37825_c1_g3_i1	collagen alpha-1(I) chain	COL1A1	-1.3	-4.4	-7.8	0.4	0.0	0.0
92	TRINITY_DN34178_c2_g1_i2	creatine kinase M-type	CKM	-6.0	-0.3	-0.8	0.0	0.8	0.7
93	TRINITY_DN37492_c0_g1_i3	C-type lectin domain family 2 member D-like isoform X1	CLEC2D	-4.5	-0.6	-0.2	0.0	0.7	1.0
94	TRINITY_DN19561_c3_g3_i1	cytochrome c oxidase assembly factor 5	COA5	-3.7	0.9	1.8	0.0	0.5	0.5
95	TRINITY_DN30220_c3_g2_i1	cytochrome c oxidase subunit I (mitochondrion)	MT-CO1	-10.7	1.0	0.9	0.0	0.4	0.7
96	TRINITY_DN25546_c6_g2_i1	cytochrome c oxidase subunit II (mitochondrion)	MT-CO2	-9.2	1.9	2.2	0.0	0.2	0.4
97	TRINITY_DN31796_c0_g2_i4	cytosolic phospholipase A2 gamma	PLA2G4C	-1.2	-3.8	-4.4	0.4	0.0	0.2
98	TRINITY_DN34475_c0_g4_i2	dehydrogenase/reductase SDR family member 7C	DHRS7C	-3.8	-0.8	-2.1	0.0	0.6	0.4

99	TRINITY_DN27718_c1_g2_i1	desmin like	DES	-3.9	-0.7	-1.6	0.0	0.6	0.6
100	TRINITY_DN37400_c1_g1_i7	desmocollin-1 isoform X1	DSC1	-0.2	-4.1	-4.7	0.9	0.0	0.1
101	TRINITY_DN38178_c1_g2_i3	DNA-binding death effector domain-containing protein 2	DEDD2	-3.6	-0.8	0.0	0.0	0.6	1.0
102	TRINITY_DN25885_c3_g1_i1	E3 ubiquitin-protein ligase TRIM63	TRIM63	3.0	4.8	-2.0	0.0	0.0	0.5
103	TRINITY_DN28739_c2_g1_i1	elongation factor 1-beta	EEF1B2	-4.5	2.2	2.2	0.0	0.1	0.4
104	TRINITY_DN36346_c1_g1_i2	endoplasmic reticulum junction formation protein lunapark isoform X1	Lnpk	-3.7	-0.4	-0.7	0.0	0.8	0.8
105	TRINITY_DN29939_c0_g1_i1	epididymal secretory protein E1	NPC2	2.9	1.4	-2.2	0.0	0.4	0.6
106	TRINITY_DN20765_c0_g1_i1	ETS-related transcription factor Elf-3	ELF3	1.6	5.0	1.0	0.6	0.0	1.0
107	TRINITY_DN37821_c1_g1_i2	eukaryotic initiation factor 4A-II	EIF4A2	-2.8	-0.1	-0.2	0.0	1.0	0.9
108	TRINITY_DN33119_c0_g1_i3	fatty acid desaturase 1-like	FADS1	1.6	5.1	-0.6	0.6	0.0	1.0
109	TRINITY_DN33871_c5_g3_i3	feather keratin B-4-like	FKER4	0.1	-4.3	-9.3	1.0	0.0	0.0
110	TRINITY_DN27663_c1_g2_i5	ferritin, higher subunit-like	FTL	-7.0	0.3	1.6	0.0	0.8	0.6
111	TRINITY_DN22711_c0_g2_i1	fish-egg lectin-like	FEL	-3.5	0.6	0.5	0.0	0.7	0.9
112	TRINITY_DN32810_c4_g1_i6	fructose-bisphosphate aldolase A	ALDA	-3.7	-1.7	2.9	0.0	0.2	0.3
113	TRINITY_DN28408_c0_g2_i2	glutamine synthetase	GLUL	3.0	1.2	-4.8	0.0	0.4	0.1
114	TRINITY_DN37527_c4_g3_i4	glyceraldehyde-3-phosphate dehydrogenase	GAPDH	-5.2	0.8	0.4	0.0	0.3	0.9
115	TRINITY_DN33097_c1_g3_i1	glycerol-3-phosphate dehydrogenase [NAD(+)], cytoplasmic	GAPD1	-3.3	0.3	-0.1	0.0	0.8	1.0
116	TRINITY_DN27794_c1_g1_i3	glycine-rich cell wall structural protein-like	GRP1	0.9	-4.6	-6.2	0.5	0.0	0.1
117	TRINITY_DN37554_c1_g1_i3	glycogen phosphorylase, liver form	PYGL	0.4	-2.6	-7.5	0.8	0.1	0.0
118	TRINITY_DN37554_c1_g1_i2	glycogen phosphorylase, muscle	PYGM	-4.3	-3.7	-4.9	0.0	0.0	0.1

		form							
119	TRINITY_DN30693_c1_g1_i3	GTPase HRas-like	HRAS	-3.6	0.2	0.5	0.0	0.9	0.9
120	TRINITY_DN28822_c3_g3_i1	heat shock cognate 71 kDa protein-like	HSPA8	-3.8	0.4	0.4	0.0	0.8	0.9
121	TRINITY_DN38168_c1_g1_i1	heat shock protein 30C-like	HSP30C	2.9	-0.8	-4.8	0.0	0.6	0.1
122	TRINITY_DN33508_c0_g1_i3	heterogeneous nuclear ribonucleoprotein H isoform X4	HNRNPH1	2.7	4.0	3.4	0.1	0.0	0.2
123	TRINITY_DN19565_c0_g2_i1	HIG1 domain family member 2A, mitochondrial	HIG2A	-3.3	1.2	1.8	0.0	0.4	0.5
124	TRINITY_DN23441_c0_g3_i6	histidine triad nucleotide-binding protein 1	HINT1	-3.7	0.8	1.5	0.0	0.6	0.6
125	TRINITY_DN35958_c1_g1_i7	inosine-5'-monophosphate dehydrogenase 1	IMPDH1	-3.5	-0.5	-1.0	0.0	0.8	0.7
126	TRINITY_DN35280_c0_g1_i2	keratin, type I cytoskeletal 10-like	KRT10	0.4	-4.1	-4.7	0.8	0.0	0.1
127	TRINITY_DN37110_c0_g1_i3	keratin, type I cytoskeletal 14-like	KRT14	2.3	4.8	-1.2	0.1	0.0	0.8
128	TRINITY_DN20271_c0_g1_i2	keratin, type I cytoskeletal 19	KRT19	-2.7	-5.2	-7.2	0.1	0.0	0.0
129	TRINITY_DN34028_c0_g1_i5	keratin, type I cytoskeletal 23-like	KRT23	0.2	-3.7	-5.6	0.9	0.0	0.1
130	TRINITY_DN20247_c0_g2_i3	keratin, type I cytoskeletal 24-like	KRT24	-0.1	-4.8	-7.4	1.0	0.0	0.0
131	TRINITY_DN37419_c0_g2_i1	keratin, type II cytoskeletal 5-like	KRT5	-3.0	-3.4	-7.0	0.0	0.0	0.0
132	TRINITY_DN37980_c1_g3_i3	keratin, type II cytoskeletal cochlear-like	KRT7	-0.3	-5.7	-9.0	0.8	0.0	0.0
133	TRINITY_DN33770_c1_g2_i1	keratin-associated protein 5-5-like	KRTAP5-5	0.4	-3.9	-0.5	0.8	0.0	0.9
134	TRINITY_DN21461_c0_g2_i2	keratin-associated protein 9-1-like	KRTAP9-1	0.7	-4.3	-2.7	0.6	0.0	0.3
135	TRINITY_DN24317_c2_g1_i3	luc7-like protein 3 isoform X1	LUC7L3	-4.0	1.0	1.3	0.0	0.5	0.6
136	TRINITY_DN30544_c0_g1_i3	ly6/PLAUR domain-containing protein 3-like	LYPD3	0.2	-5.6	-2.3	0.9	0.0	0.4
137	TRINITY_DN30209_c0_g2_i1	lymphocyte antigen 6E-like	Ly6a	0.4	-3.7	-2.7	0.8	0.0	0.3
138	TRINITY_DN29603_c0_g1_i4	MAPK regulated corepressor interacting protein 2	MCRIP2	2.9	2.1	-1.6	0.0	0.2	0.7
139	TRINITY_DN26604_c2_g2_i6	microtubule-associated proteins	MAP1LC3B	3.7	1.0	-0.6	0.0	1.0	1.0

		1A/1B light chain 3B							
140	TRINITY_DN35142_c1_g2_i2	mitochondrial uncoupling protein 3	UCP3	1.2	4.0	-2.6	0.5	0.0	0.5
141	TRINITY_DN34043_c1_g1_i3	myc box-dependent-interacting protein 1 isoform X6	BIN1	-2.9	-0.6	-1.1	0.0	0.7	0.7
142	TRINITY_DN37316_c3_g1_i4	myc box-dependent-interacting protein 1 isoform X8	BIN1	-5.0	1.0	0.9	0.0	0.5	0.7
143	TRINITY_DN31785_c1_g2_i6	myelin P2 protein-like	PMP2	2.3	-4.2	-4.8	0.1	0.0	0.1
144	TRINITY_DN30564_c1_g1_i4	myoblast determination protein 1	MYOD1	-3.3	0.5	1.0	0.0	0.7	0.7
145	TRINITY_DN38080_c1_g1_i2	myomesin-1 isoform X1	MYOM1	-2.1	-3.7	-4.3	0.2	0.0	0.2
146	TRINITY_DN34011_c0_g1_i1	myosin heavy chain, skeletal muscle, adult	MYH1	-1.0	-4.6	-7.0	0.5	0.0	0.0
147	TRINITY_DN34714_c1_g1_i2	myosin light chain 1/3, skeletal muscle isoform isoform X2	MYL1	-5.3	0.8	0.1	0.0	0.5	1.0
148	TRINITY_DN23319_c0_g1_i6	myosin light polypeptide 6 isoform X2	MYL6	-3.2	0.7	1.2	0.0	0.7	0.6
149	TRINITY_DN23306_c0_g2_i1	myosin regulatory light chain 2, ventricular/cardiac muscle isoform	MYL2	-0.5	-4.4	1.1	0.7	0.0	0.7
150	TRINITY_DN38338_c2_g2_i3	myosin-1B-like isoform X2	MYO1B	-0.9	-3.8	-6.2	0.5	0.0	0.1
151	TRINITY_DN38343_c2_g1_i2	myosin-1B-like isoform X4	MYO1B	0.2	-0.8	-6.7	0.9	0.6	0.0
152	TRINITY_DN38338_c1_g1_i3	myosin-1B-like isoform X4 like	MYO1B	-3.1	-3.3	-2.5	0.0	0.0	0.4
153	TRINITY_DN26737_c2_g1_i1	myosin-3-like isoform X7	MYH3	-5.5	1.2	0.5	0.0	0.3	0.9
154	TRINITY_DN30527_c1_g1_i1	myosin-7B isoform X2	MYH7B	-3.0	1.1	0.1	0.0	0.5	1.0
155	TRINITY_DN37664_c0_g1_i2	myosin-binding protein C, fast-type	MYBPC2	-3.6	0.1	-0.1	0.0	1.0	1.0
156	TRINITY_DN32432_c1_g1_i3	myozenin-1 isoform X1	MYOZ1	-3.6	0.3	0.0	0.0	0.9	1.0
157	TRINITY_DN21082_c0_g1_i3	NADH dehydrogenase [ubiquinone] 1 subunit C2	NDUFC2	-5.1	1.2	1.8	0.0	0.4	0.5
158	TRINITY_DN21927_c2_g5_i1	NADH dehydrogenase subunit 5 (mitochondrion)	NDUFV2	5.2	4.7	1.7	0.0	0.0	0.6

159	TRINITY_DN38263_c1_g1_i3	nebulin isoform X34	NEB	-0.9	-3.7	-4.8	0.5	0.0	0.1
160	TRINITY_DN16072_c1_g1_i3	Similar to Apteryx australis mantelli genome assembly AptMant0	N/A	-4.0	-1.1	-1.3	0.0	0.5	0.6
161	TRINITY_DN18856_c0_g1_i1	Scavenger receptor class B member 2 S homeolog (scarb2.S), mRNA	SCARB2	2.0	4.0	1.0	0.4	0.0	1.0
162	TRINITY_DN18900_c1_g6_i1	Keratin-associated protein 4-8-like (LOC107109571), mRNA	KRTAP4-8	4.2	2.0	1.0	0.0	0.4	1.0
163	TRINITY_DN20555_c2_g2_i3	Zinc finger protein 239-like (LOC107181380), mRNA	ZFP239	2.8	3.3	3.7	0.1	0.0	0.2
164	TRINITY_DN20594_c5_g1_i3	Similar to Scarelus anthracinus voucher UPOL NG0053 NADH dehydrogenase subunit 5 (ND5) gene	ND5	-4.1	0.4	1.2	0.0	0.8	0.7
165	TRINITY_DN20871_c1_g2_i1	Cathepsin Z (CTSZ)	CTSZ	0.7	-4.5	-5.7	0.6	0.0	0.1
166	TRINITY_DN20937_c1_g4_i2	Solute carrier family 38 member 5 (SLC38A5)	SLC38A5	-3.7	1.4	1.8	0.0	0.3	0.5
167	TRINITY_DN21620_c1_g1_i3	Monocarboxylate transporter 1-like (LOC107125559), mRNA	SLC16A1	3.5	2.0	-0.6	0.0	0.4	1.0
168	TRINITY_DN22245_c1_g1_i2	Cyclic AMP-dependent transcription factor ATF-2	ATF2	-0.6	3.5	2.2	1.0	0.0	0.5
169	TRINITY_DN23291_c3_g7_i1	Calsequestrin-1 like	CASQ1	-8.4	0.3	0.1	0.0	0.9	1.0
170	TRINITY_DN23323_c1_g1_i1	Parvalbumin (PVALB), mRNA	PVALB	3.0	1.6	-3.8	0.0	0.3	0.3
171	TRINITY_DN23920_c1_g2_i2	WD repeat and SOCS box containing 1 (WSB1),	WB1	-5.2	1.1	1.4	0.0	0.4	0.6
172	TRINITY_DN24078_c2_g1_i1	Ring finger protein 24 (RNF24), transcript variant X1, mRNA	RNF24	1.4	-4.3	-4.9	0.3	0.0	0.1
173	TRINITY_DN24197_c1_g1_i1	KIS(5-71) SINE Squam1, complete sequence	Squam1	3.9	-1.0	0.7	0.0	1.0	0.9
174	TRINITY_DN24202_c0_g4_i2	Similar to Gekko japonicus	SLN	-8.5	1.0	-0.6	0.0	0.5	0.8

		sarcopin (SLN), transcript variant X1							
175	TRINITY_DN24910_c2_g3_i9	Plasmolipin (PLLP), mRNA	PLLP	2.9	0.4	-2.2	0.0	1.0	0.6
176	TRINITY_DN26094_c0_g2_i6	Similar to Cyprinus carpio genome assembly common carp genome	N/A	0.7	-5.8	-2.1	0.6	0.0	0.4
177	TRINITY_DN26203_c0_g1_i1	Similar to Drosophila ficusphila sodium/potassium/calcium exchanger Nckx30C	Nckx30C	-4.2	1.0	0.4	0.0	0.5	0.9
178	TRINITY_DN26440_c3_g2_i2	Erythrocyte membrane protein band 4.1 (EPB41), transcript variant X13, mRNA	EPB41	6.0	3.7	-0.6	0.0	0.0	1.0
179	TRINITY_DN26576_c1_g1_i1	DOT1 like histone lysine methyltransferase (DOT1L)	DOT1L	-3.8	1.1	1.6	0.0	0.4	0.6
180	TRINITY_DN27369_c1_g4_i1	Ring finger protein 20 (RNF20), mRNA	RNF20	-4.2	1.5	2.5	0.0	0.3	0.4
181	TRINITY_DN27386_c1_g1_i4	ATPase inhibitory factor 1 (ATPIF1)	ATPIF1	-5.2	0.9	1.8	0.0	0.5	0.5
182	TRINITY_DN27804_c1_g2_i1	Glutamate receptor interacting protein 2	GRIP2	0.0	4.2	0.0	1.0	0.0	1.0
183	TRINITY_DN27804_c1_g2_i5	Solute carrier family 6 (neurotransmitter transporter), member 6 (SLC6A6), transcript variant X3, mRNA	SLC6A6	3.3	0.7	-2.2	0.0	0.8	0.6
184	TRINITY_DN27900_c1_g1_i3	Premature ovarian failure, 1B (POF1B)	POF1B	-4.6	1.4	2.1	0.0	0.4	0.4
185	TRINITY_DN27971_c0_g2_i2	Lymphocyte antigen 86 (LY86), transcript variant X1, mRNA	LY86	3.5	-0.6	-2.2	0.0	1.0	0.6
186	TRINITY_DN28000_c3_g1_i2	28S ribosomal RNA	RPS28	-4.3	0.4	0.3	0.0	0.8	0.9
187	TRINITY_DN28023_c1_g1_i1	Xin actin-binding repeat-containing protein 2-like	XIRP2l	-6.8	0.8	1.3	0.0	0.6	0.6

188	TRINITY_DN28063_c0_g2_i3	Myozenin 3 (MYOZ3)	MYOZ3	-3.7	-0.1	-1.7	0.0	1.0	0.5
189	TRINITY_DN28124_c0_g5_i6	Tropomyosin 1 (TPM1), transcript variant X5,	TPM1	-5.3	-0.1	-0.4	0.0	0.9	0.9
190	TRINITY_DN29368_c2_g1_i1	similar to Podarcis muralis uncharacterized LOC114586692 (LOC114586692), ncRNA	LOC114586692	1.3	-5.0	-7.1	0.4	0.0	0.0
191	TRINITY_DN30390_c1_g1_i1	Myc box-dependent-interacting protein 1	BIN1	-4.1	0.3	0.3	0.0	0.9	0.9
192	TRINITY_DN30395_c0_g1_i5	Keratin, type II cytoskeletal 1	KRT1	-3.5	-3.2	-7.1	0.0	0.0	0.0
193	TRINITY_DN30509_c0_g1_i2	Calcium/calmodulin dependent protein kinase II gamma (CAMK2G)	CAMK2G	-3.5	0.3	0.3	0.0	0.9	0.9
194	TRINITY_DN30512_c2_g1_i4	Fermitin family member 2 (FERMT2), transcript variant X4, mRNA	FERMT2	3.5	2.3	-0.6	0.0	0.3	1.0
195	TRINITY_DN30587_c0_g2_i1	Uncharacterized	N/A	-2.9	1.2	1.6	0.0	0.4	0.6
196	TRINITY_DN30884_c0_g2_i1	FANCD2/FANCI-associated nuclease 1 (FAN1)	FAN1	-4.7	0.9	1.1	0.0	0.5	0.7
197	TRINITY_DN31847_c0_g3_i1	Cold inducible RNA binding protein	CIRBP	-3.7	0.5	1.5	0.0	0.7	0.6
198	TRINITY_DN32104_c3_g1_i3	Integrin subunit beta 2 (ITGB2), mRNA	ITGB2	3.3	-3.7	-4.3	0.0	0.0	0.2
199	TRINITY_DN32564_c0_g2_i1	CD63 molecule (CD63), transcript variant X2, mRNA	CD63	3.2	2.5	1.2	0.0	0.1	0.8
200	TRINITY_DN32941_c3_g1_i2	Triosephosphate isomerase 1 (TPI1), mRNA	TPI1	1.5	1.0	-6.9	0.3	0.5	0.0
201	TRINITY_DN33871_c5_g3_i1	Similar to Hemidactylus turcicus mRNA for ge-gprp4	gpr4	-0.4	-3.8	2.1	0.8	0.0	0.5
202	TRINITY_DN34416_c0_g3_i1	Centromere-associated protein E (LOC108000233), transcript variant X2	CENPE	-4.1	0.7	1.2	0.0	0.7	0.7

203	TRINITY_DN34551_c1_g1_i2	Unconventional myosin-XVI-like	MYO16	-4.8	1.9	0.1	0.0	0.2	1.0
204	TRINITY_DN35421_c1_g1_i4	Xin actin binding repeat containing 2 (XIRP2)	XIRP2	-4.0	-0.3	-1.1	0.0	0.8	0.7
205	TRINITY_DN36311_c0_g2_i1	Homocysteine-inducible, endoplasmic reticulum stress-inducible, ubiquitin-like domain member 1 (HERPUD1)	HERPUD1	-3.5	-0.1	1.3	0.0	1.0	0.6
206	TRINITY_DN37045_c0_g1_i3	Unknown open reading frame, human C8orf22 (LOC107107199), mRNA	C8orf22	4.5	2.8	-2.6	0.0	0.1	0.5
207	TRINITY_DN37251_c1_g5_i2	Calpain small subunit 1	CAPNS1	-3.5	0.6	1.7	0.0	0.7	0.5
208	TRINITY_DN37466_c1_g3_i1	NDRG1 protein	NDRG1	-1.0	3.8	0.4	1.0	0.0	1.0
209	TRINITY_DN37517_c6_g2_i2	Parvalbumin beta-like (LOC107123052), mRNA	N/A	3.4	3.4	1.8	0.1	0.0	0.5
210	TRINITY_DN37631_c0_g1_i1	Similar to Gopherus evgoodei uncharacterized LOC115654989	N/A	-5.2	0.3	0.4	0.0	0.9	0.9
211	TRINITY_DN37929_c1_g1_i4	Methylthioadenosine phosphorylase (MTAP)	MTAP	-7.3	0.2	-1.2	0.0	0.9	0.7
212	TRINITY_DN38030_c0_g2_i3	Autophagy-related protein 9A-like (LOC107118613), transcript variant X6, mRNA	ATG9A	3.0	1.3	-1.6	0.0	0.4	0.7
213	TRINITY_DN38294_c1_g2_i2	Periostin (POSTN), transcript variant X12	POSTN	-3.0	1.6	0.9	0.0	0.3	0.7
214	TRINITY_DN38304_c1_g2_i1	Collagen type III alpha 1 chain (COL3A1)	COL3A1	-1.6	-5.4	-0.1	0.2	0.0	1.0
215	TRINITY_DN35262_c0_g1_i1	ornithine decarboxylase antizyme 2	OAZ2	-4.3	0.2	0.8	0.0	0.9	0.8
216	TRINITY_DN36464_c1_g1_i6	pancreatic progenitor cell differentiation and proliferation factor-like protein	PPDPFL	5.0	2.2	-1.6	0.0	0.2	0.8
217	TRINITY_DN29832_c0_g2_i2	PDZ and LIM domain protein 5	PDLIM5	-5.4	0.4	-1.0	0.0	0.8	0.7

		isoform X2							
218	TRINITY_DN33680_c0_g2_i5	PDZ and LIM domain protein 7 isoform X4	PDLIM7	-7.4	0.2	-0.4	0.0	0.9	0.9
219	TRINITY_DN27621_c0_g2_i4	peptidyl-prolyl cis-trans isomerase FKBP3	FKBP3	-3.6	1.5	1.3	0.0	0.3	0.6
220	TRINITY_DN29857_c1_g1_i1	phosphoglycerate kinase 1	PGK1	-3.3	0.3	-0.2	0.0	0.8	0.9
221	TRINITY_DN37070_c1_g3_i1	plakophilin-1	PKP1	-1.5	-3.8	-4.4	0.3	0.0	0.2
222	TRINITY_DN28295_c1_g2_i3	polyubiquitin-B isoform X1	UBB	3.6	2.5	-0.6	0.0	0.1	0.9
223	TRINITY_DN30180_c0_g1_i2	probable ATP-dependent RNA helicase DDX17	DDX17	-1.2	-3.8	-4.4	0.4	0.0	0.2
224	TRINITY_DN24163_c0_g2_i1	probable peroxisomal membrane protein PEX13	PEX13	3.6	0.0	0.4	0.0	1.0	1.0
225	TRINITY_DN35520_c1_g2_i4	proline dehydrogenase 1, mitochondrial-like	PRODH	3.4	1.8	-1.6	0.0	0.2	0.6
226	TRINITY_DN28789_c0_g1_i4	protein FAM162A	FAM162A	-3.6	0.5	1.6	0.0	0.8	0.5
227	TRINITY_DN31243_c0_g1_i1	protein FAM184B	FAM184B	3.7	1.6	-0.6	0.0	0.6	1.0
228	TRINITY_DN36144_c0_g1_i4	protein kinase C and casein kinase substrate in neurons protein 2-like isoform X1	PACSIN2	-3.6	-1.0	-1.2	0.0	0.5	0.7
229	TRINITY_DN28763_c0_g4_i1	protein SET	SET	-3.2	1.1	1.6	0.0	0.4	0.5
230	TRINITY_DN37046_c1_g1_i4	pyruvate kinase PKM isoform X1	PKM	-4.0	-0.8	-1.5	0.0	0.6	0.6
231	TRINITY_DN28890_c1_g2_i9	regulator of cell cycle RGCC-like	RGCC	2.0	3.7	2.2	0.4	0.0	0.6
232	TRINITY_DN37687_c1_g1_i5	RNA-binding protein 24	RBM24	-3.6	0.2	-0.1	0.0	0.9	1.0
233	TRINITY_DN38335_c0_g1_i1	ryanodine receptor 1	RYR1	-3.8	-3.6	-5.2	0.0	0.0	0.1
234	TRINITY_DN38019_c1_g3_i2	sarcoplasmic/endoplasmic reticulum calcium ATPase 1	ATP2A1	-4.5	-0.4	-1.1	0.0	0.8	0.7
235	TRINITY_DN29632_c0_g2_i2	serpin B10-like	SERPINB10	0.9	-6.9	-2.4	0.5	0.0	0.4
236	TRINITY_DN30685_c0_g2_i5	S-formylglutathione hydrolase	ESD	-3.8	1.1	1.0	0.0	0.5	0.7
237	TRINITY_DN35169_c0_g3_i1	SH3 domain-binding glutamic acid-rich protein	SH3BGR	-3.5	0.0	-1.7	0.0	1.0	0.5

238	TRINITY_DN29450_c0_g3_i3	sphingomyelin phosphodiesterase 5	smpd5	1.0	3.9	1.0	1.0	0.0	1.0
239	TRINITY_DN19422_c0_g1_i2	thioredoxin domain-containing protein 17	TXNDC17	0.0	-0.9	-7.4	1.0	0.5	0.0
240	TRINITY_DN38339_c2_g2_i1	titin isoform X10	TTN	-1.4	-4.9	-8.3	0.3	0.0	0.0
241	TRINITY_DN25133_c0_g1_i11	trans-1,2-dihydrobenzene-1,2-diol dehydrogenase	DHDH	1.1	-3.8	-5.3	0.4	0.0	0.1
242	TRINITY_DN37409_c0_g1_i2	transitional endoplasmic reticulum ATPase	VCP	-3.6	-0.1	-0.2	0.0	1.0	1.0
243	TRINITY_DN37819_c2_g1_i8	translationally-controlled tumor protein	TPT1	-3.2	1.1	1.3	0.0	0.5	0.6
244	TRINITY_DN28724_c0_g2_i2	transmembrane protein 223	TMEM223	2.3	3.8	2.4	0.2	0.0	0.5
245	TRINITY_DN37095_c3_g2_i3	triosephosphate isomerase	TPI1	-3.7	-0.6	-0.2	0.0	0.7	0.9
246	TRINITY_DN37172_c0_g2_i2	tripartite motif-containing protein 72	TRIM72	2.8	1.1	-2.9	0.0	0.5	0.4
247	TRINITY_DN31007_c0_g2_i5	tropomodulin-4	TMOD4	-3.8	0.7	0.2	0.0	0.6	1.0
248	TRINITY_DN32390_c3_g1_i2	tropomyosin alpha-3 chain isoform X1	TPM3	-4.5	0.6	0.0	0.0	0.7	1.0
249	TRINITY_DN38292_c1_g1_i4	troponin I, fast skeletal muscle	TNNI2	-9.3	1.4	0.3	0.0	0.3	0.9
250	TRINITY_DN28063_c1_g1_i2	troponin I, slow skeletal muscle	TNNI1	-3.5	1.2	0.8	0.0	0.4	0.8
251	TRINITY_DN24287_c5_g2_i1	troponin T, fast skeletal muscle isoform X1	TNNT3	-5.9	1.0	0.0	0.0	0.4	1.0
252	TRINITY_DN27210_c1_g2_i1	ubiquitin-60S ribosomal protein L40	UBA52	-4.7	1.2	1.7	0.0	0.4	0.5
253	TRINITY_DN30472_c0_g1_i3	vitamin D3 hydroxylase-associated protein-like	VDHAP	-3.2	1.0	0.2	0.0	0.5	0.9
254	TRINITY_DN38095_c1_g1_i2	zinc finger protein 106 isoform X1	ZNF106	-1.2	-4.0	-4.6	0.4	0.0	0.2

Table 2: List of differentially expressed protein based on iTRAQ proteomic analysis. Accession, description, symbol, No of peptides identified, peptide sequence matches, 1dpa fold changes, 2dpa fold changes, 5dpa fold changes, 1dpa SEM, 2dpa SEM and 5dpa SEM were shown in each column.

S.No	Accession	Description	Symbol	# Peptides	# PSMs	1DPA	2DPA	5DPA	SEM1	SEM2	SEM5
1	TRINITY_DN23220_c0_g2_i4	hemoglobin subunit beta	HBB	3	3	3.85	2.79	-0.85	0.29	0.68	0.59
2	TRINITY_DN34721_c0_g1_i1	myosin-binding protein H	MYBPH	1	1	3.17	0.32	-1.82	0.13	0.13	0.19
3	TRINITY_DN19815_c3_g1_i2	hemoglobin subunit alpha-D	HBAD	2	4	3.13	1.66	-1.74	0.66	0.76	0.50
4	TRINITY_DN31561_c0_g6_i1	S100-A7-like	S100A7	3	5	2.86	0.29	-0.66	0.21	2.34	4.06
5	TRINITY_DN23557_c1_g5_i3	TRINITY_DN23557_c1_g5_i3	N/A	1	1	2.85	-1.45	-3.66	0.16	0.22	0.33
6	TRINITY_DN22863_c0_g2_i2	histone H2A.Z	H2AFZ	4	8	2.68	1.34	-0.39	1.08	0.73	0.15
7	TRINITY_DN36348_c1_g1_i1	Annexin A2	ANXA2	4	7	2.20	1.06	-0.37	0.46	0.34	0.54
8	TRINITY_DN33300_c0_g3_i5	TRINITY_DN33300_c0_g3_i5	N/A	8	12	2.19	1.36	-0.48	0.05	0.21	0.25
9	TRINITY_DN36487_c0_g2_i1	cathepsin B	CTSB	1	2	2.05	0.07	-1.83	0.18	0.06	0.03
10	TRINITY_DN34850_c1_g2_i1	mimecan	OGN	4	6	2.03	-0.06	-2.48	0.06	0.32	0.73
11	TRINITY_DN29980_c3_g2_i1	myosin light chain 1/3, skeletal muscle isoform isoform X2	MYL1	6	10	1.95	1.51	-0.97	0.56	0.40	0.41
12	TRINITY_DN23998_c0_g1_i3	tubulin beta chain	TUBB	5	6	1.80	0.89	-1.08	0.20	0.24	0.03
13	TRINITY_DN23258_c0_g1_i1	histone H2B 5	H2B-V	2	4	1.79	-0.06	-1.59	0.74	0.81	0.82
14	TRINITY_DN36141_c1_g1_i2	L-lactate dehydrogenase A chain	LDHA	8	10	1.76	1.09	-2.44	0.73	0.63	2.83
15	TRINITY_DN26001_c2_g1_i2	alpha-actinin-1 isoform X1	ACTN1	2	2	1.70	1.13	-0.68	0.37	0.45	0.29
16	TRINITY_DN25724_c1_g3_i3	vimentin	VIM	6	6	1.68	1.00	-0.97	0.61	0.43	0.38
17	TRINITY_DN38128_c1_g2_i3	myosin-binding protein C, slow-type isoform X6	MYBPC1	7	13	1.64	0.99	-0.55	2.45	0.45	0.77
18	TRINITY_DN12736_c0_g1_i1	apolipoprotein A-I	APOA1	5	10	1.64	-0.63	-2.25	0.20	0.50	0.73
19	TRINITY_DN36902_c2_g1_i2	alcohol dehydrogenase 1	Adh1	1	1	1.63	1.74	-1.76	0.05	0.02	0.04

20	TRINITY_DN26228_c0_g1_i7	short chain dehydrogenase gsfK-like	GSFK	1	1	1.63	-2.24	-5.82	0.03	0.25	0.34
21	TRINITY_DN36364_c0_g1_i7	tubulin alpha-1A chain	TUBA1A	4	4	1.62	0.86	-1.22	0.72	0.71	0.64
22	TRINITY_DN37921_c1_g2_i2	keratin, type I cytoskeletal 24-like	KRT24	8	8	1.6	1.4	-0.5	0.61	0.58	0.07
23	TRINITY_DN34661_c0_g1_i3	phosphoglucomutase-1 isoform X2	PGM1	7	11	1.55	1.58	-1.01	0.46	0.23	0.07
24	TRINITY_DN27002_c0_g1_i1	actin, cytoplasmic 2	ACTG1	21	48	1.52	1.19	-0.44	0.69	0.53	0.30
25	TRINITY_DN32459_c0_g1_i1	calpain small subunit 1	CAPNS1	1	1	1.52	-0.46	-4.13	0.08	0.03	1.27
26	TRINITY_DN21930_c0_g2_i3	Proteasome subunit beta type-2	PSMB2	1	1	1.45	-0.72	-2.97	0.11	0.02	0.14
27	TRINITY_DN20734_c0_g4_i1	Actin alpha cardiac muscle 1	ACTC1	23	65	1.41	1.57	-1.00	0.53	0.37	0.36
28	TRINITY_DN34313_c0_g1_i4	ATP synthase subunit alpha, mitochondrial	ATP1	2	2	1.35	0.53	-1.18	0.02	0.04	0.09
29	TRINITY_DN29508_c0_g1_i2	TRINITY_DN29508_c0_g1_i2	N/A	1	1	1.31	0.91	-1.34	0.10	0.06	0.08
30	TRINITY_DN37043_c2_g2_i2	creatine kinase M-type	CKM	9	16	1.28	1.04	-1.61	0.60	0.58	0.42
31	TRINITY_DN27922_c3_g1_i4	adenylate kinase isoenzyme 1 isoform X1	AK1	3	6	1.26	-0.39	-1.29	1.00	0.73	0.42
32	TRINITY_DN33300_c0_g3_i4	TRINITY_DN33300_c0_g3_i4	N/A	13	22	1.26	0.56	-1.68	0.54	0.56	0.72
33	TRINITY_DN36070_c0_g2_i4	LIM domain-binding protein 3 isoform X12	LDB3	2	2	1.15	0.30	-1.17	0.25	0.14	0.40
34	TRINITY_DN28295_c1_g2_i4	polyubiquitin-C	UBC	1	1	1.14	2.13	-0.29	0.84	0.76	0.15
35	TRINITY_DN37255_c1_g2_i2	leukotriene A-4 hydrolase	LKA4	1	1	1.13	1.51	0.23	0.22	0.25	0.11
36	TRINITY_DN38343_c2_g2_i1	myosin-1B-like isoform X5	MYO1B	35	60	1.08	1.45	-1.12	1.15	0.31	0.56
37	TRINITY_DN34296_c3_g8_i1	actin, alpha cardiac muscle 1	ACTC1	15	43	1.07	1.23	-0.58	0.36	0.42	0.41
38	TRINITY_DN23035_c0_g2_i2	dihydrolipoyl dehydrogenase, mitochondrial	DLD	3	3	1.1	0.5	-0.7	0.98	0.76	0.06
39	TRINITY_DN33310_c0_g1_i2	histone H2A type 2-B-like	HIST2H2AB	1	1	1.07	-0.88	-1.71	1.09	0.84	0.50
40	TRINITY_DN38292_c1_g1_i4	troponin I, fast skeletal muscle	TNNI2	4	5	1.06	0.77	-0.96	1.27	0.42	0.50
41	TRINITY_DN32404_c3_g1_i6	actin aortic smooth muscle	ACTA2	19	53	1.06	0.61	-1.32	0.62	0.28	0.33
42	TRINITY_DN30191_c0_g7_i1	F-actin-capping protein subunit beta isoform X2	CAPZB	1	1	1.00	-0.30	-3.88	0.05	0.06	0.14
43	TRINITY_DN28501_c1_g1_i4	synaptic vesicle membrane protein VAT-1 homolog	VAT1	1	1	0.99	0.32	-1.00	0.03	0.10	0.04

44	TRINITY_DN28891_c0_g1_i2	malate dehydrogenase, mitochondrial	MDH2	2	2	0.98	0.00	-2.67	0.06	0.11	0.36
45	TRINITY_DN32432_c1_g2_i2	myozenin-1 isoform X1	MYOZ1	4	5	1.0	1.1	-1.2	0.6	0.6	0.3
46	TRINITY_DN28342_c0_g1_i2	myosin heavy chain, skeletal muscle-like	MYH	9	13	0.97	1.56	-0.36	1.05	0.42	0.45
47	TRINITY_DN27358_c0_g1_i3	glutathione S-transferase-like	GST	2	2	0.92	-1.65	-4.33	0.14	0.31	0.03
48	TRINITY_DN27718_c1_g2_i1	desmin	DES	4	5	0.92	0.42	-0.87	0.44	0.23	0.13
49	TRINITY_DN36557_c1_g1_i2	fructose-bisphosphate aldolase C	ALDOC	5	7	0.86	0.88	-1.57	0.62	0.29	1.06
50	TRINITY_DN22922_c0_g1_i4	galectin-3 isoform X2	LGALS3	1	1	0.81	-0.34	-2.48	0.00	0.08	0.09
51	TRINITY_DN34182_c1_g1_i1	TRINITY_DN34182_c1_g1_i1	N/A	20	68	0.80	0.93	-0.54	0.63	0.42	0.28
52	TRINITY_DN22784_c0_g1_i2	TRINITY_DN22784_c0_g1_i2	N/A	13	20	0.79	0.15	-3.16	0.55	0.37	0.81
53	TRINITY_DN29857_c1_g1_i1	phosphoglycerate kinase 1	PGK1	3	4	0.8	0.8	-1.0	0.03	0.07	0.02
54	TRINITY_DN37459_c2_g1_i2	alpha-actinin-2 isoform X1	LOC100179322	16	17	0.77	1.79	-0.15	0.88	0.75	0.72
55	TRINITY_DN37078_c1_g1_i8	cytosol aminopeptidase	LAP3	1	1	0.69	1.59	0.63	0.34	0.44	0.21
56	TRINITY_DN33047_c0_g1_i1	heat shock protein HSP 90-alpha	HSP90AA1	2	2	0.68	0.86	-0.62	0.94	0.04	0.01
57	TRINITY_DN37032_c0_g2_i1	heat shock cognate 71 kDa protein	HSPA8	1	1	0.67	0.85	-0.92	0.93	0.57	0.45
58	TRINITY_DN34564_c0_g1_i6	annexin A6 isoform X1	ANXA6	1	1	0.64	0.80	-0.93	0.81	0.77	0.25
59	TRINITY_DN28342_c0_g2_i2	heat shock cognate 71 kDa protein-like	HSPA8	2	2	0.61	0.90	-0.54	0.82	0.42	0.12
60	TRINITY_DN38304_c0_g1_i4	TRINITY_DN38304_c0_g1_i4	N/A	1	1	0.60	-0.22	-2.08	1.16	0.06	1.17
61	TRINITY_DN29028_c0_g2_i3	phosphoglycerate mutase 1	PGAM1	6	8	0.58	1.12	0.31	0.54	1.05	0.23
62	TRINITY_DN27789_c2_g1_i2	phosphoglycerate mutase 2	PGAM2	5	12	0.54	-0.16	-3.49	0.02	0.10	0.06
63	TRINITY_DN26466_c0_g2_i5	Protein O-GlcNAcase	OGA	10	16	0.50	0.64	0.12	0.39	0.32	0.48
64	TRINITY_DN36562_c0_g1_i9	glutathione S-transferase Mu 1-like	GSTM1	2	4	0.49	-0.01	-1.11	0.31	0.12	0.55
65	TRINITY_DN31350_c0_g1_i3	peroxiredoxin-6	PRDX6	1	1	0.49	-0.63	-3.76	0.03	0.01	0.28
66	TRINITY_DN28781_c0_g1_i3	pyruvate kinase PKM isoform X2	PKM	1	1	0.47	0.77	-0.55	1.45	0.86	0.28
67	TRINITY_DN37517_c6_g2_i1	parvalbumin beta	PVALB	3	3	0.46	1.66	-1.51	0.31	1.30	0.51

68	TRINITY_DN26606_c2_g2_i1	F-actin-capping protein subunit alpha-2	CAPZA2	1	1	0.45	-0.39	-3.42	0.07	0.08	0.01
69	TRINITY_DN37046_c1_g1_i4	pyruvate kinase PKM isoform X1	PKM	6	6	0.45	1.01	-0.96	0.58	0.33	0.39
70	TRINITY_DN33370_c2_g2_i3	keratin, type II cytoskeletal 5-like	KRT5	7	8	0.4	0.8	-0.6	0.15	0.31	0.29
71	TRINITY_DN34011_c0_g1_i3	myosin-1B-like isoform X2	MYO1B	2	3	0.44	0.83	-4.91	0.00	0.01	0.05
72	TRINITY_DN29832_c0_g2_i2	PDZ and LIM domain protein 5 isoform X2	PDLIM5	2	3	0.39	-0.64	-3.40	0.14	0.14	0.20
73	TRINITY_DN37554_c1_g1_i2	glycogen phosphorylase, muscle form	PYGM	16	27	0.38	0.70	-1.66	0.50	0.34	0.45
74	TRINITY_DN22345_c2_g1_i1	Parvalbumin alpha	PVALB	2	3	0.37	1.78	-0.06	1.18	0.55	0.97
75	TRINITY_DN29856_c0_g1_i2	carbonyl reductase [NADPH] 1-like	CBR1	1	1	0.33	-0.65	-3.32	0.04	0.09	0.15
76	TRINITY_DN34096_c0_g1_i3	aldose reductase-like	AR	2	3	0.33	-0.49	-3.31	0.03	0.03	0.27
77	TRINITY_DN38029_c0_g1_i4	collagen alpha-1(I) chain	COL1A1	26	30	0.28	-0.18	-0.45	0.28	0.81	1.02
78	TRINITY_DN37645_c3_g2_i1	myosin regulatory light chain 2, skeletal muscle isoform	MYLPF	2	4	0.26	2.91	-0.65	0.05	0.07	0.10
79	TRINITY_DN22413_c0_g2_i1	N-acetylneuraminase lyase	NPL	3	6	0.18	1.11	0.86	0.30	0.92	0.91
80	TRINITY_DN32810_c4_g1_i4	fructose-bisphosphate aldolase A	ALDOA	8	35	0.18	1.34	-0.71	0.41	0.42	0.52
81	TRINITY_DN32365_c1_g2_i2	myozenin-3	MYOZ3	1	1	0.11	-0.55	-3.38	0.07	0.10	0.27
82	TRINITY_DN37786_c0_g1_i2	collagen alpha-1(VI) chain	COL6A1	5	5	0.04	0.21	-1.95	0.22	0.47	1.20
83	TRINITY_DN34741_c2_g2_i1	heat shock protein HSP 90-beta	HSP90AB1	2	2	0.03	0.81	-1.10	0.11	0.08	0.08
84	TRINITY_DN26737_c2_g1_i1	myosin-3-like isoform X7	MYH3	12	17	-0.01	1.09	-0.84	0.74	0.17	0.62
85	TRINITY_DN33401_c0_g2_i2	complement component 1 Q subcomponent-binding protein, mitochondrial	C1QBP	1	1	-0.02	-0.30	-2.58	0.03	0.02	0.17
86	TRINITY_DN29973_c3_g1_i6	troponin T, fast skeletal muscle isoform X1	TNNT3	3	10	-0.08	-0.24	-3.64	0.35	0.07	0.34
87	TRINITY_DN37310_c1_g1_i4	plectin isoform X4	PLEC1	1	1	-0.08	0.45	-0.76	0.00	0.04	0.04
88	TRINITY_DN37095_c3_g2_i3	triosephosphate isomerase	TPI1	8	14	-0.09	-0.34	-5.37	1.20	0.52	0.70
89	TRINITY_DN29661_c3_g1_i3	tropomyosin alpha-3 chain isoform X1	TPM3	7	8	-0.17	-0.11	-4.27	0.19	0.03	0.06

90	TRINITY_DN35037_c0_g1_i3	glucose-6-phosphate isomerase	GPI	3	3	-0.18	0.54	-0.90	0.39	0.12	0.05
91	TRINITY_DN37574_c0_g1_i1	ubiquitin-like modifier-activating enzyme 1	UBA1	1	1	-0.18	1.09	-1.11	0.03	0.07	0.07
92	TRINITY_DN35510_c0_g1_i3	myelin basic protein isoform X2	MBP	2	3	-0.21	0.29	-1.88	0.86	0.65	0.86
93	TRINITY_DN32170_c0_g3_i2	glycerol-3-phosphate dehydrogenase [NAD(+)], cytoplasmic	GPD1	2	2	-0.23	-0.37	-3.79	0.62	0.38	0.01
94	TRINITY_DN37021_c1_g1_i5	alpha-enolase isoform X1	ENO1	12	17	-0.23	1.01	-1.30	0.75	0.60	0.32
95	TRINITY_DN16558_c0_g2_i1	collagen alpha-3(VI) chain isoform X10	COL6A3	1	1	-0.23	0.37	-2.25	0.44	0.44	0.43
96	TRINITY_DN37508_c1_g1_i1	collagen alpha-2(I) chain	COL1A2	14	18	-0.27	-0.43	-2.40	0.54	0.84	0.08
97	TRINITY_DN28227_c0_g1_i2	ADP/ATP translocase 3	SLC25A6	1	1	-0.32	0.49	-1.24	0.03	0.00	0.07
98	TRINITY_DN37706_c0_g3_i4	periostin isoform X1	POSTN	3	3	-0.35	0.77	-1.38	0.04	0.03	0.31
99	TRINITY_DN36097_c0_g1_i2	nebulin	NEB	2	2	-0.40	0.45	-1.22	0.03	0.02	0.28
100	TRINITY_DN26034_c1_g1_i1	transitional endoplasmic reticulum ATPase-like	VCP	1	1	-0.42	0.80	-0.85	0.14	0.08	0.20
101	TRINITY_DN18038_c1_g2_i1	collagen alpha-1(XV) chain isoform X1	COL15A1	1	2	-0.44	0.65	-1.92	0.14	0.03	0.10
102	TRINITY_DN37512_c1_g1_i6_	hydroperoxide isomerase ALOXE3-like	ALOXE3	2	4	-0.5	0.2	-1.7	0.28	0.30	0.08
103	TRINITY_DN35151_c1_g3_i3	desmocollin-1 isoform X1	DSC1	1	5	-0.54	0.28	-0.72	0.22	0.20	0.36
104	TRINITY_DN18988_c0_g3_i1	titin-like isoform X23	TTN	2	2	-0.55	0.72	-1.28	0.19	0.16	0.12
105	TRINITY_DN37493_c2_g1_i1	myosin-7B isoform X2	MYH7B	16	30	-0.61	0.60	-0.50	0.09	0.02	0.71
106	TRINITY_DN38339_c2_g3_i1	titin isoform X19	TTN	9	11	-0.6	0.8	-1.6	0.05	0.13	0.23
107	TRINITY_DN38338_c2_g1_i4	myosin-7-like	MYH7	6	7	-0.62	-0.10	1.22	0.07	0.62	0.25
108	TRINITY_DN38296_c2_g1_i3_	ryanodine receptor 1	RYR1	1	1	-0.6	0.8	-1.0	0.01	0.05	0.32
109	TRINITY_DN38142_c2_g2_i1	myomesin-2	MYOM1	6	7	-0.66	0.35	-1.61	0.02	0.07	0.08
110	TRINITY_DN37478_c0_g1_i2	glyceraldehyde-3-phosphate dehydrogenase 2	GAPDHS	8	8	-0.67	0.03	-3.11	0.57	0.30	0.90
111	TRINITY_DN19098_c0_g1_i1	collagen alpha-2(VI) chain isoform X1	COL6A2	2	3	-0.67	0.72	-0.73	0.03	0.11	0.03
112	TRINITY_DN38157_c0_g1_i1	myomesin-1 isoform X2	MYOM1	2	2	-0.72	0.62	-1.58	0.02	0.00	0.00
113	TRINITY_DN36747_c0_g1_i5	AMP deaminase 1	AMPD1	2	2	-0.78	0.46	-0.70	0.01	0.01	0.11

114	TRINITY_DN38132_c4_g1_i1	sarcoplasmic/endoplasmic reticulum calcium ATPase 1 isoform X2	ATP2A1	16	21	-0.80	0.77	-1.72	0.02	0.05	0.02
115	TRINITY_DN38343_c2_g1_i2	myosin-1B-like isoform X4	MYO1B	19	42	-0.8	1.3	-2.1	0.11	0.32	0.17
116	TRINITY_DN25656_c0_g1_i1	myosin-3 isoform X1	MYH3	12	16	-0.89	0.97	-1.44	0.03	0.01	0.05
117	TRINITY_DN37664_c1_g1_i1	myosin-binding protein C, fast-type	MYBPC2	8	10	-0.95	1.01	-1.13	0.77	0.14	0.12
118	TRINITY_DN37754_c1_g1_i3	synaptophysin-like protein 2	SYPL2	1	2	-0.96	0.69	-2.25	0.03	0.01	0.13
119	TRINITY_DN38316_c1_g1_i3	nebulin isoform X9	NEB	14	15	-1.05	-0.16	-1.30	0.25	0.39	0.30
120	TRINITY_DN36517_c0_g2_i1	ATP-dependent 6-phosphofructokinase, muscle type	PFKM	10	14	-1.06	0.71	-1.32	0.02	0.02	0.04
121	TRINITY_DN38333_c1_g1_i1	glycogen debranching enzyme isoform X1	AGL	1	1	-1.09	0.74	-1.60	0.04	0.03	0.02
122	TRINITY_DN34542_c0_g1_i4	ovotransferrin-like isoform X1	TF	3	3	-1.12	2.41	-0.36	0.21	0.19	0.16
123	TRINITY_DN34011_c0_g1_i1	myosin heavy chain, skeletal muscle, adult	MYH1	6	11	-1.34	1.52	-2.63	0.37	0.23	0.16
124	TRINITY_DN27696_c0_g2_i4	alpha-2-macroglobulin-like	A2M	2	2	-1.61	2.11	-1.23	1.10	0.76	0.04
125	TRINITY_DN34296_c3_g4_i1	actin, cytoplasmic 2	ACTB	1	1	-1.85	-0.34	-1.16	0.01	0.04	0.04
126	TRINITY_DN28457_c0_g1_i3	titin isoform X50	TTN	2	2	-2.32	1.72	-1.89	0.04	0.04	0.09
127	TRINITY_DN33871_c5_g3_i3	feather keratin B-4-like	FKER	2	4	-3.19	0.85	-0.68	0.63	0.11	0.08
128	TRINITY_DN31256_c2_g1_i3	glyceraldehyde-3-phosphate dehydrogenase	GAPDH	5	10	-4.97	1.26	-1.78	0.62	0.39	1.10

Figure 1:

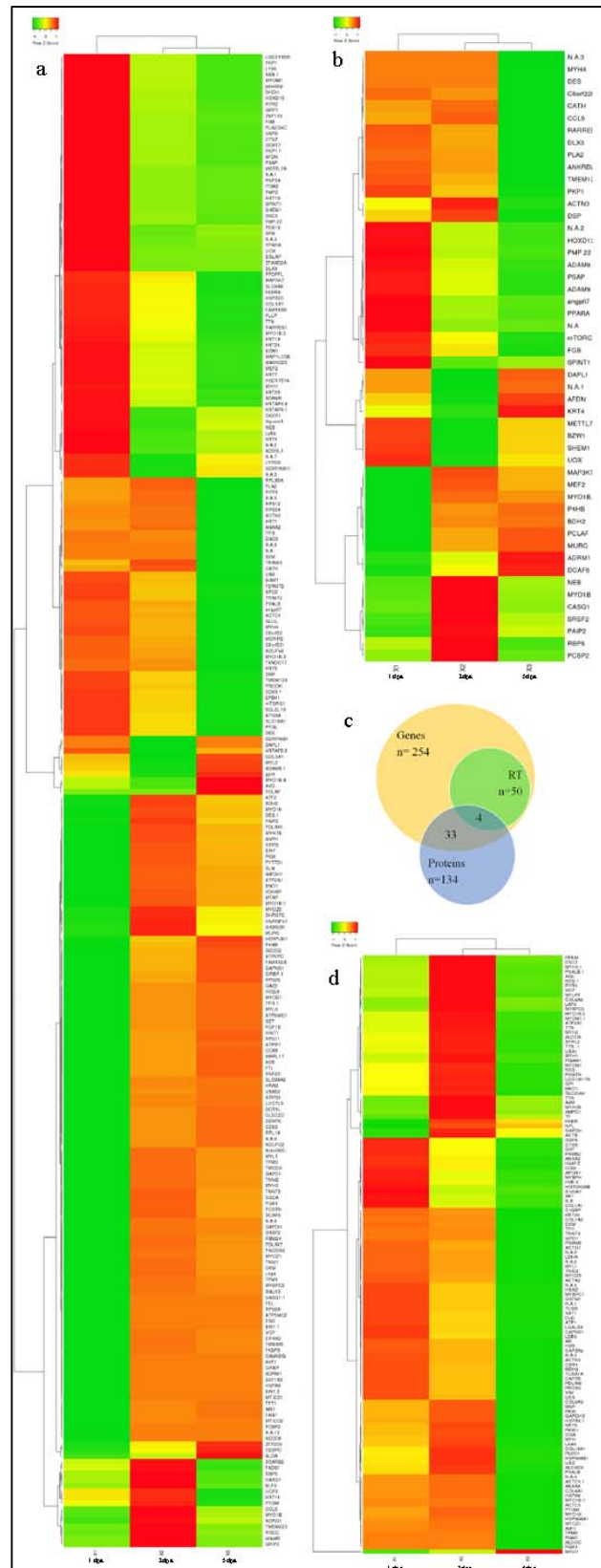


Figure 2:

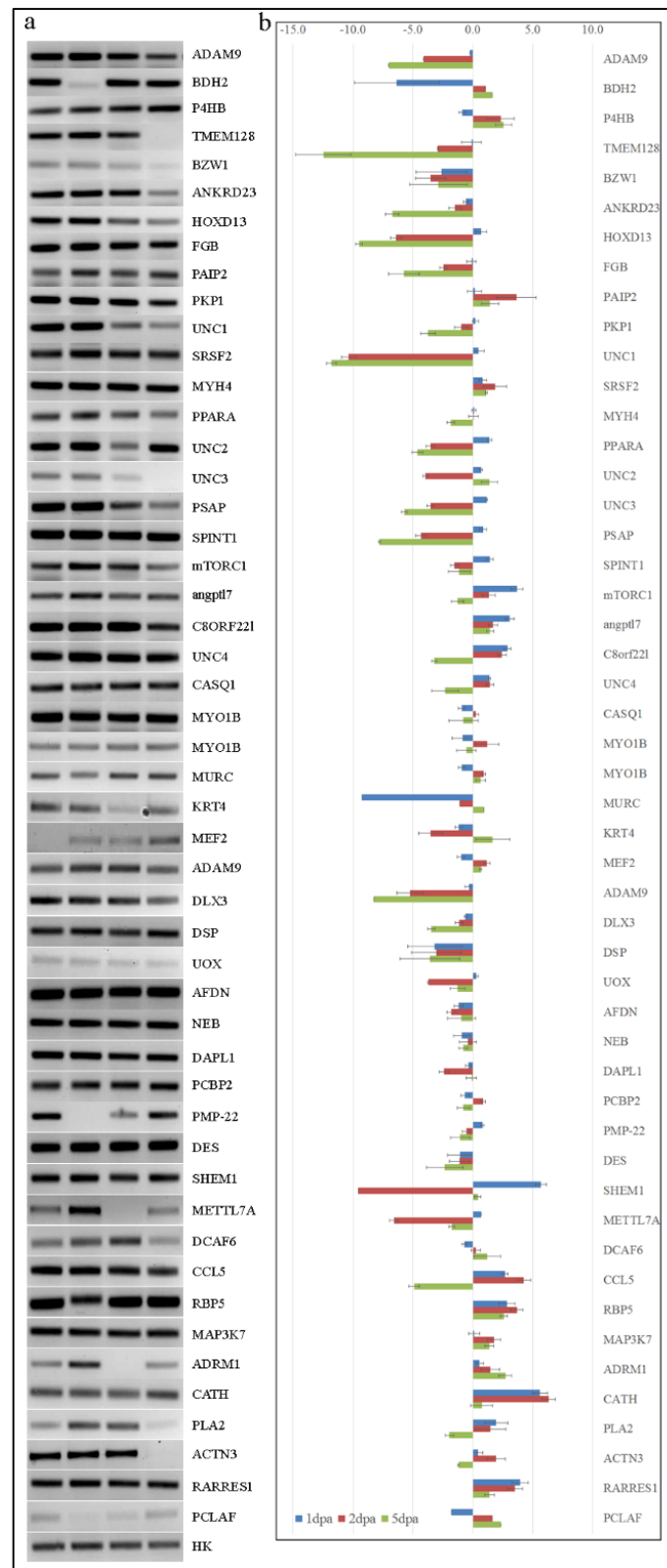
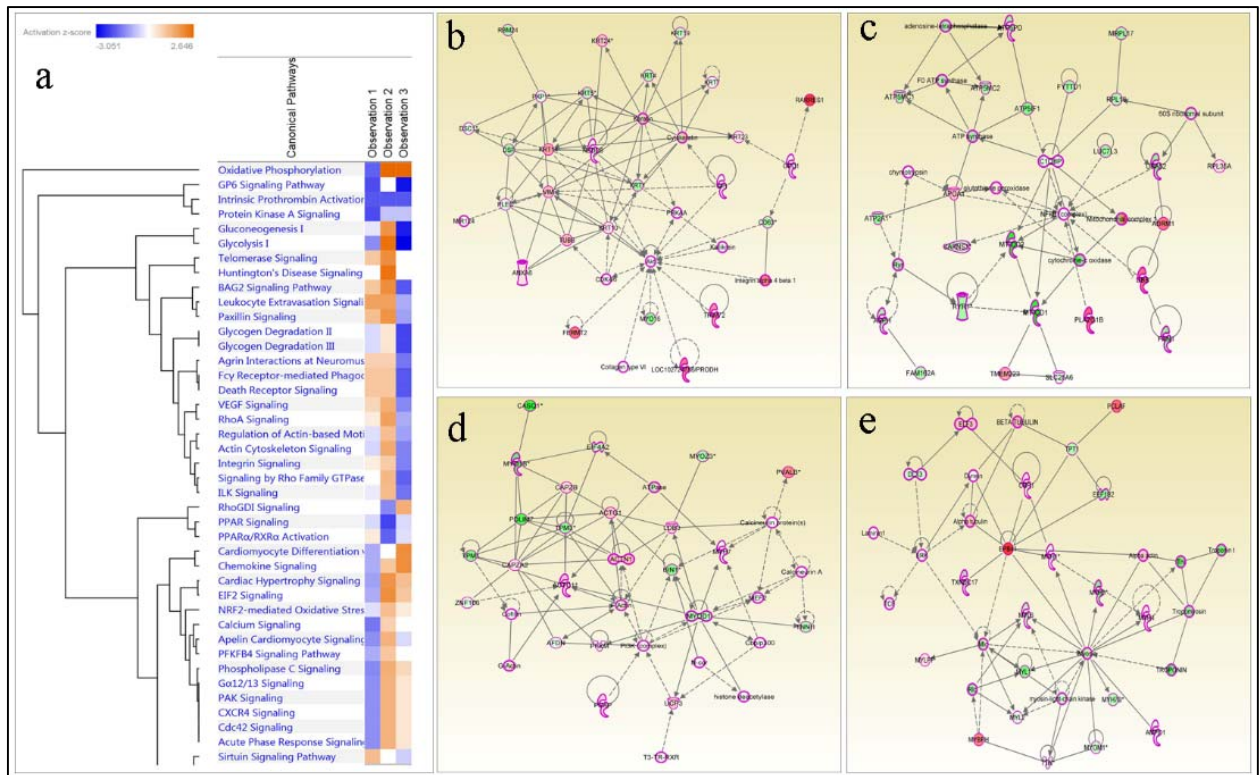
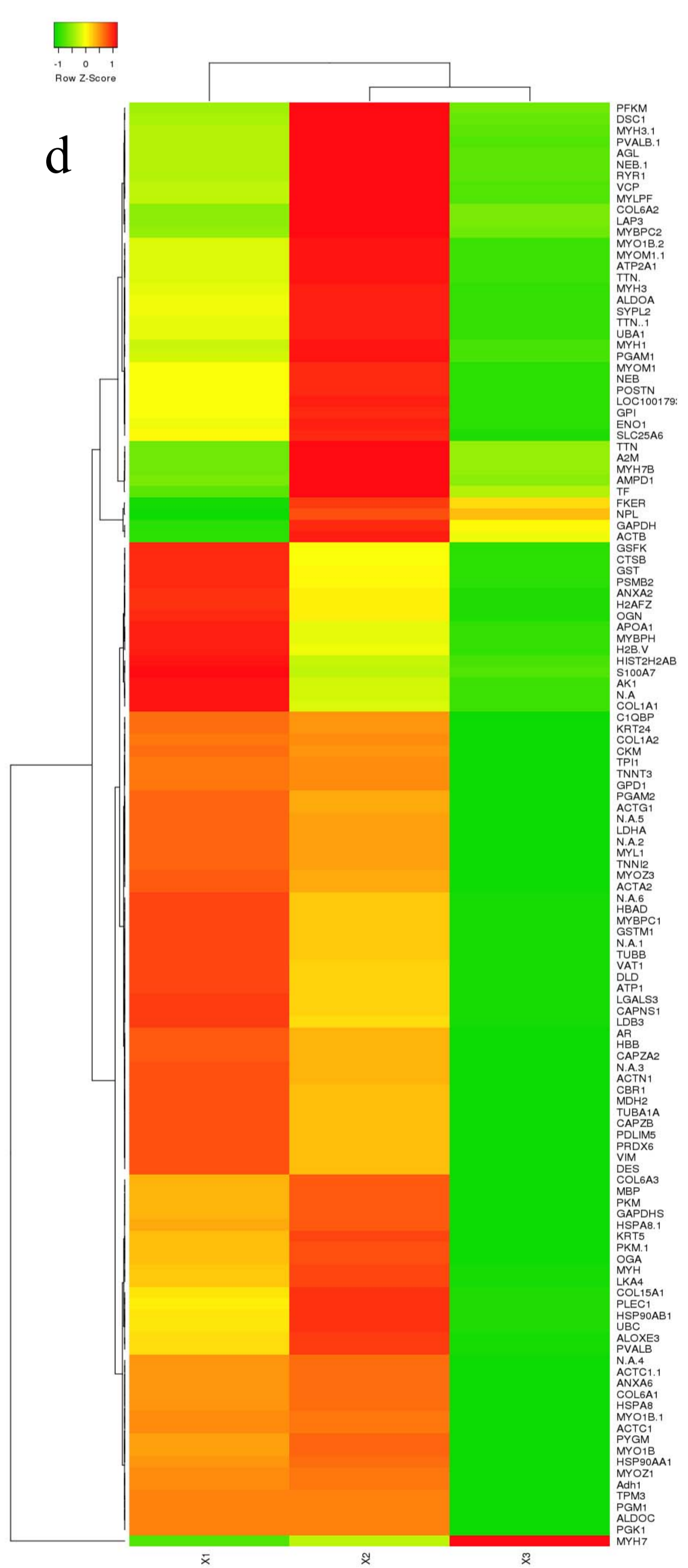
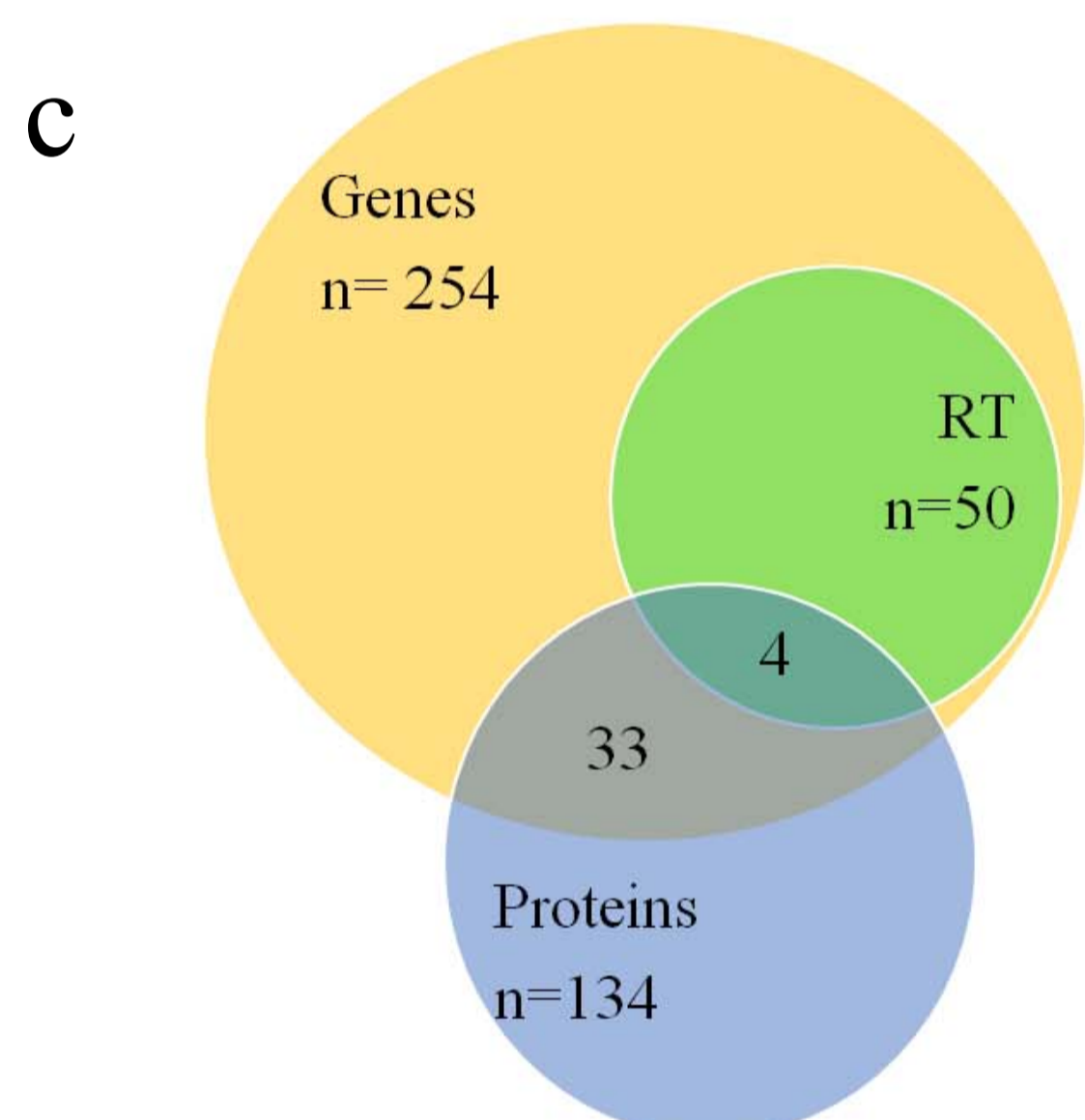
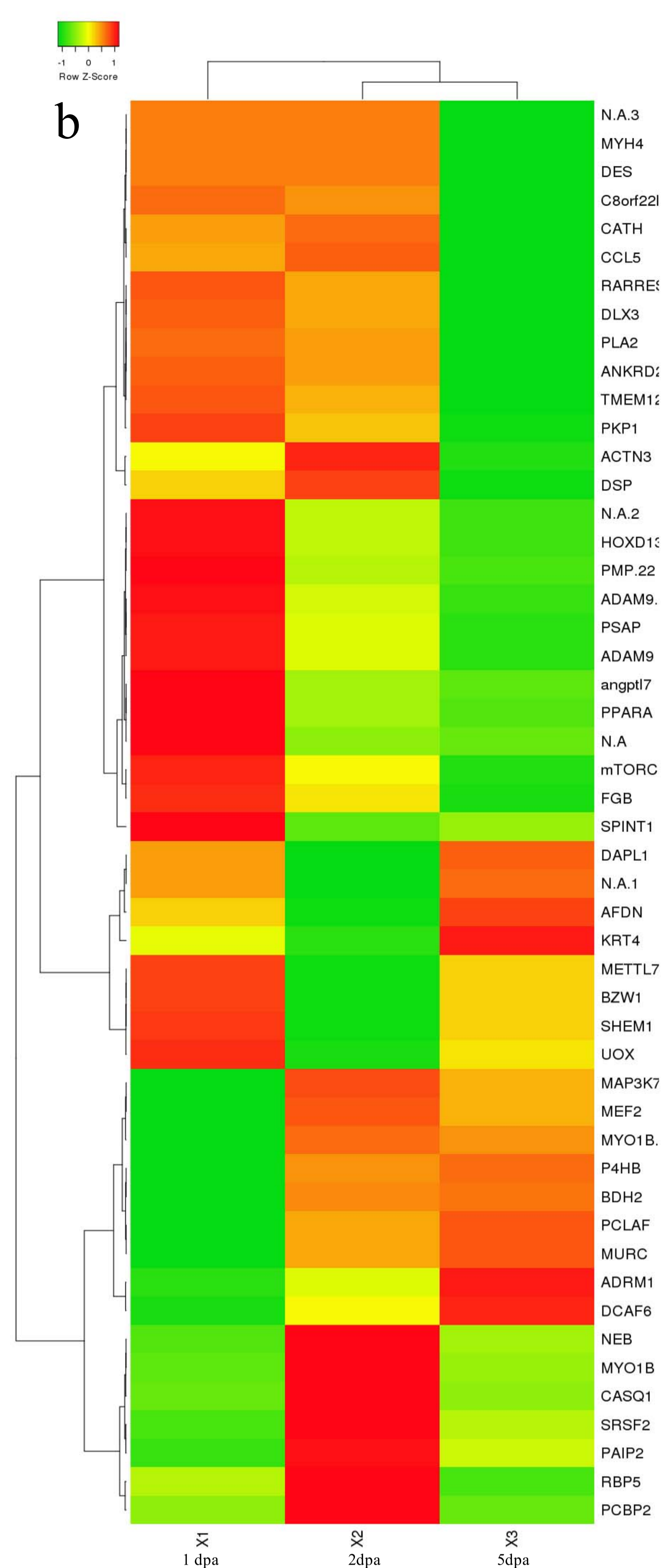
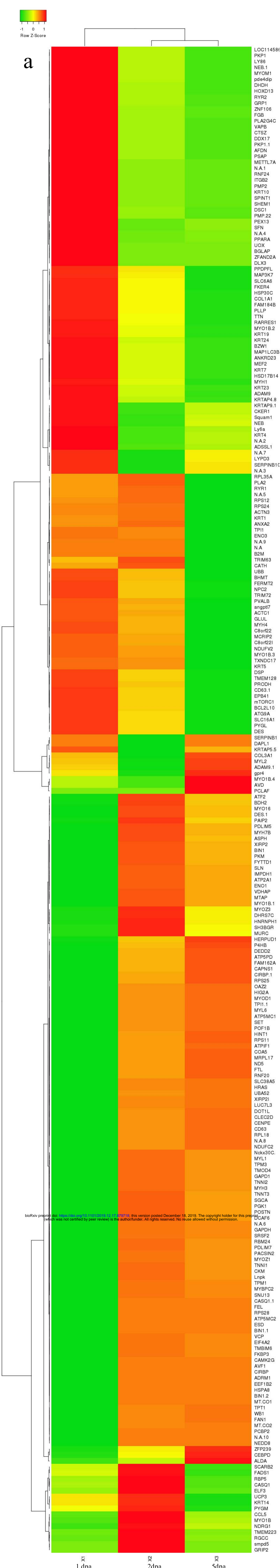
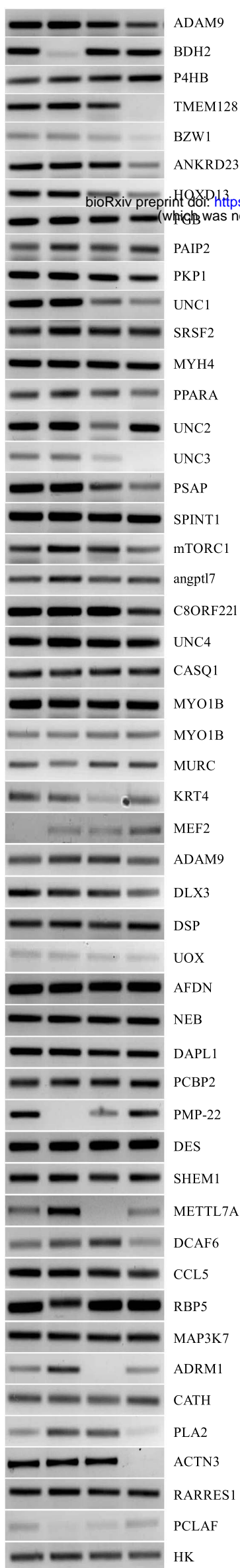
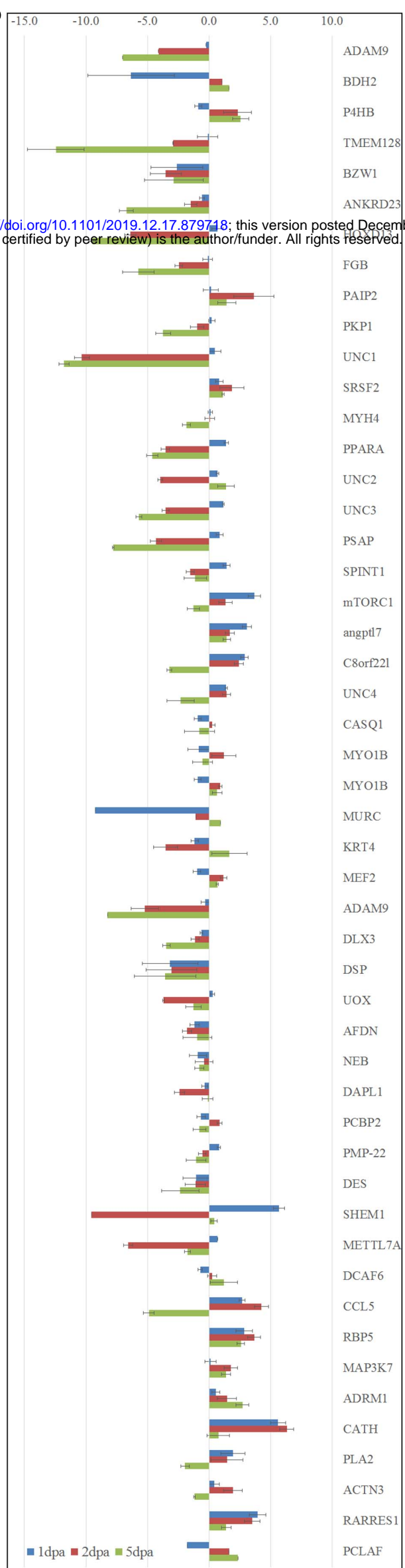


Figure 3:





a**b**

bioRxiv preprint doi: <https://doi.org/10.1101/2019.12.17.879718>; this version posted December 18, 2019. The copyright holder for this preprint (which was not certified by peer review) is the author/funder. All rights reserved. No reuse allowed without permission.

